Chapter 1

Minimal Energy Paths on the Terrain

1.1 Introduction

While Euclidean shortest paths on terrain surfaces provide optimal length paths, they do not generally provide optimal time/energy paths since they ignore the terrain attributes. Weighted shortest paths provide more realism in that they can incorporate some terrain attributes such as variable costs for different regions, face slopes and/or frictional coeficients. However, these different weight costs are constant for each region (face) and therefore they ignore the very important issue of travel direction. The direction of travel plays a large role in determining the physical effects incurred on a vehicle (i.e., car, truck, robot, person, etc...) travelling along a terrain surface. It is for this reason that we investigate *anisotropic* paths (i.e. paths that take into account the direction of travel as well as length and weight). Through anisotropism, we can also identify certain directions of travel that represent inclines that are too steep to ascend or unsafe to travel due to possible dangers such as overturning, sliding or wheel slippage. We address the problem of determining a path for a vehicle between two points, s and t, on a terrain $\mathcal{P}$ such that the path minimizes energy consumption and does not travel on "dangerous" slopes.

The chapter is organized as follows. We first introduce the physical model (weight metric) that is used to determine the cost of an anisotropic path. We then discuss some of the properties of the paths that obey this special anisotropic weight metric. Third, we explain how the anisotropic paths can be approximated in a straight forward and potentialy practical manner and then give bounds on the approximation produced. We then describe an improved scheme, namely an ϵ-approximation with a better worst-case bound. Lastly, we discuss a possible improvement to the model and the effects that it has on our algorithms.

1.2 The Physical Model

We've chosen the model of Rowe and Ross [6] for solving our shortest energy path problem. The model allows two main forces to act against the propulsion of the vehicle, namely that of friction and gravity. We assume that the vehicle has no net acceleration over the path from s to t and that the cost of turning is insignificant w.r.t. energy loss. Hence the model ignores the cost and feasibility of making turns.

We assume that $\mathcal{P}$ is composed of n triangular faces, each face $f_j, 1 \leq j \leq n$ having a homogeneous weight (cost) μ_j pertaining to the coeficient of kinetic friction (between 0 and 1) for that face w.r.t. the moving vehicle. Examples of some coefficients are shown in Table 1.2 for different types of scenarios. The rubber on concrete, for example, may be used to represent vehicle movement on roadways. In some scenarios, it may be desirable to have more than one coefficient of friction assigned to each face. For example, modelling a person climbing up a hill (face) may require a coefficient simillar to "rubber shoes on snow" and that person coming down the hill may use a snowboard which would require a different coefficient such as "waxed wood on dry snow" (see Table 1.2). We will assume in our model that only one coefficent is assigned to each face which will be used for both uphill and downhill traversal.

Scenario	μ_j
rubber on concrete	0.8
wood on wood	0.2
waxed wood on dry snow	0.04
ice on ice	0.03

Table 1.1: Some known coefficents of friction.

1.2.1 Basic Model (Weight Metric)

Let mg be the weight of the vehicle. Now consider a segment s_i of the shortest path which crosses a face f_j of $\mathcal{P}$. Let ϕ_j be the inclination angle (gradient) of f_j and let φ_i be the inclination angle of s_i w.r.t. the XY plane (see Figure 1.1). Our model assumes that the terrain has no vertical faces and so it is always the case that $-90 < \phi_j, \varphi_i < 90$. Our model assumes that the cost of travel for s_i is:

$$mg(\mu_j \cos\phi_j + \sin\varphi_i) \cdot |s_i| \tag{1.1}$$

We assume that mg is constant for the problem instance and hence we will multiply the obtained path cost by this factor after it has been computed. The cost due to the force of friction is represented by $\mu_j \cos\phi_j \cdot |s_i|$. Rowe and Ross [6] reason about paths in their 2-D azimuth projections on the plane of the 2.5D terrain. They ignore the $\cos\phi_j$ factor, stating that it is very close to 1 for most traversable natural terrain. We keep this value since it is easily computed and can be combined with the μ_j factor to get an overall face weight. Therefore, we will define $w_j = \mu_j \cos\phi_j$ to be the weight of face f_j.

The cost due to gravity is represented by $|s_i|\sin\varphi_i$. It is easily seen from Figure 1.1 that this is nothing other than the change in elevation of the path segment. Hence the work expended against gravity is none other that the sum of the elevation changes of all the path segments; and this turns out to be the difference in height between s and t which is independent of the path taken. As a result, we can leave this portion out when computing the shortest cost path and add it after the path has been computed. The following is ignored with this model:

- internal energy losses (such as heat loss in an engine)
- friction of wheels on axels and wind resistance

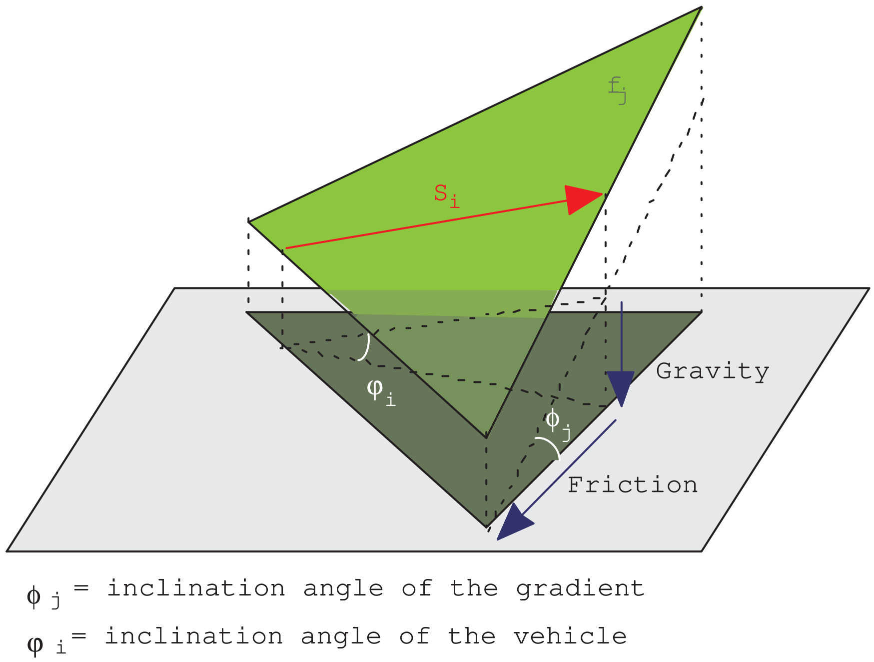

Figure 1.1: The forces of friction and gravity that act against the propulsion of the vehicle.

- costs of turning

Rowe and Ross [6] claim that internal energy losses are proportional to external work done against friction and gravity and can be handled by an appropriate multiplication factor. Also, the wheel friction and wind resistance can be modelled proportional to the path distance.

Consequently, the "uphill" anisotropic cost of travel through a face that we are interested in when computing our paths is: $w_j|s_i|$. Notice that this cost is the same as that of the weighted isotropic shortest path cost. We will now consider the effects of braking phenomenon and invalid directions (obstacles).

1.2.2 Model With Braking

For certain inclination angles, the cost formula of 1.1 becomes negative (i.e., $\varphi_i < -arcsin(\mu_j \cos\phi_j)$) and the vehicle gains energy going downhill, resulting in vehicle acceleration. This gain in energy is unrealistic in practice so we will make a modification to the model in order to ensure a positive cost metric. It is assumed that sufficient braking is applied such that there is no net acceleration when the vehicle travels downhill. Furthermore, it will be assumed that braking requires negligible energy. Hence the cost of travel during downhill braking should be zero. The change from the "uphill" formula and this new "downhill" formula will occur at the inclination angles (denoted as *critcal braking angles* defined by $\varphi_i = -\arcsin(\mu_j \cos\phi_j)$.

By replacing the $\mu_j \cos\phi_j$ friction factor by $-\sin\varphi_i$ we cancel out the gravity force resulting in zero cost travel. Notice that although the cost for downhill braking is zero, the negative gravity force has already been extracted from the metric, leaving a cost of $-\sin\varphi_i \cdot |s_i|$ for segment s_i.

This cost however, will always be positive and non-zero for the valid range of downhill angles: $-90 < \varphi_i < 0$ degrees. Therefore, downhill segments are always assigned a positive, non-zero weight.

Property 1.2.1 *For a braking segment s_i passing through face f_j, $-\sin\varphi_i \geq w_j$.*

1.2.3 Model With Anisotropic Obstacles

One last characteristic of the model is that it will avoid travel in "unsafe" directions. Rula and Nuttall [7] indicate that four conditions can give anisotropic slope limitations:

- Limited expendible force to counteract friction and gravity effects. Here the travelling inclination angle φ_i cannot exceed $\arcsin(\frac{F_{max}}{mg\sqrt{\mu_j^2+1}}) - \arctan(\mu_j)$ where F_{max} is the maximum force that the vehicle can exert.
- Speed or power limitations of the vehicle. Here the travelling inclination angle φ_i cannot exceed $\arcsin(\frac{P_{max}}{v_{min}mg\sqrt{\mu_j^2+1}}) - \arctan(\mu_j)$ where P_{max} is the maximum power that the vehicle can exert and v_{min} is the minimum (non-zero) speed of the vehicle.
- Loss of traction danger (slippage). This occurs when the travelling inclination angle φ_i exceeds approximately $\arctan(\mu'_j - \mu_j)$, where μ'_j is the coefficient of static friction of face f_j.
- Sideslope overturn danger. Here the projection of the center of gravity falls outside the polygon formed by its support points (most often perpendicular to "uphill"). The formula here depends on the vehicle shape (see Figure 1.2).

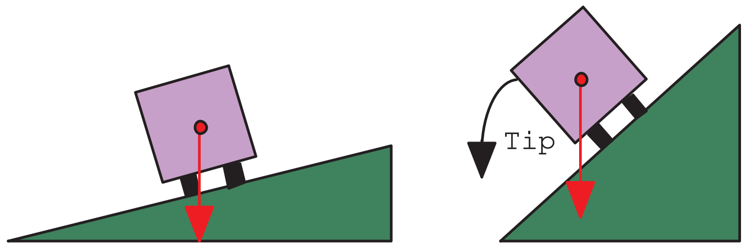

Figure 1.2: The sideslope overturn problem. The vehicle tips as its center of gravity projection falls outside the support polygon defined by the wheels.

The formulae above give rise to possibly 3 ranges of angles that define directions on a face that are impermissible for travelling. Together, with the braking range, there are up to 4 important angular ranges per face as shown in Figure 1.3. The boundary angles of the impermissible ranges are called *critical impermissibility angles*. The boundary angles of the braking range are called *critical braking angles*. For the regular angular ranges (i.e. not impremissible or braking), the range is bounded by critical impermissibility or braking angles. We will also think of these as the critical angles for the regular range. Note that in the case of very steep angles, an impermissible range may arise within the braking range due to dangers of wheel slippage. That is, some ranges of downward traversal may be too steep for safe travel. We will ignore this impermissible range, since the face itself should be deemed unsafe of travel anyway. A path is said to be *valid* if and only if it does not travel in any impermissible directions.

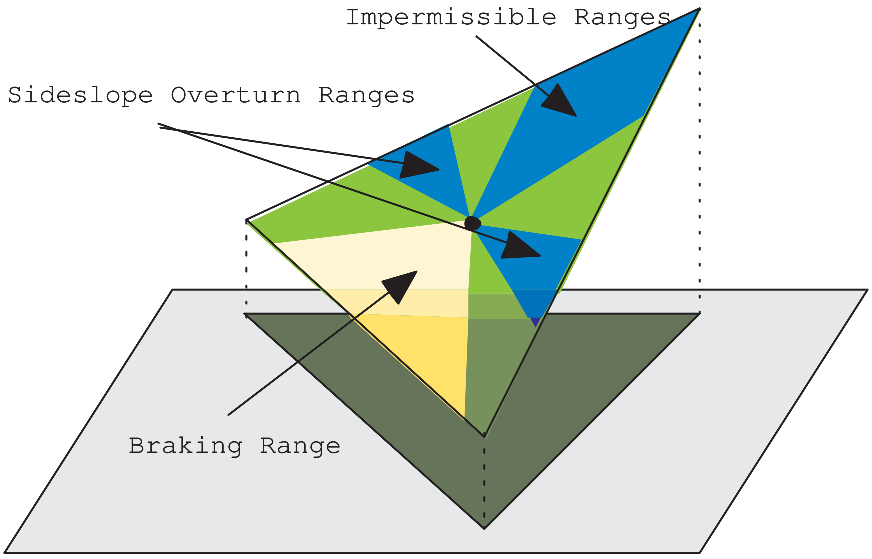

Figure 1.3: The up to 3 ranges representing impermissible travel and the braking range of a single face.

If any of the impermissible ranges overlap, they are combined to make a single impermissible range. In some cases, the ranges may cover all possible angles. This represents an *isotropic obstacle* which is essentially a face that cannot be travelled on safely. If there exists an isotropic obstacle on the $\mathcal{P}$ then it is possible that a valid path between two arbitrary points on $\mathcal{P}$ does not exist. For example, consider the example of Figure1.4. It shows that there may be no path from s to t due to the steep faces (i.e. isotropic obstacles) that surround the plateau containing t.

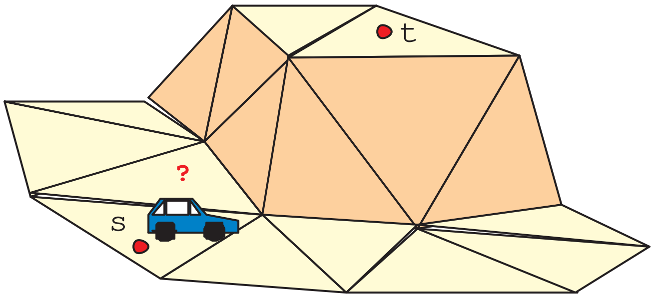

Figure 1.4: An example showing that there may notbe any valid path between two points on $\mathcal{P}$ due to isotropic obstacles (shown as steep slopes surrounding the plateau containing t).

Property 1.2.2 *Given two points s and t on $\mathcal{P}$, there may not be a valid path $\Pi(s,t)$ between s*

and t on $\mathcal{P}$.

The algorithm description and analysis presented here will assume that there exists at least one valid path (i.e. $\Pi(s,t)$) between s and t. Although we make this assumption in the analysis, our algorithm is able to detect the absence of valid paths and report when such a path does not exist. All that remains to be shown is that if a valid path does indeed exist, then our algorithm will always produce a valid path as well. We will prove this later for each of the algorithms.

Let φ_c be a critical impermissibility angle for one of the critical impermissibility ranges of a face $f_j, 1 < j < n$ of $\mathcal{P}$. Let $\vec{u}$ and $\vec{v}$ be the two unit vectors representing the directions on the boundaries of the range. Thus, the angle that $\vec{u}$ and $\vec{v}$ make with the horizontal plane is φ_c. Let α_c be the angle between these two vectors when placed end-to-end as shown in Figure 1.5. Let α_j be the minimum of all α_c for the (up to 3) impermissible ranges. Furthermore, let α be the minimum of all $\alpha_j, 1 < j < n$. Similarly, we define β as being the minimum of all $\beta_j, 1 < j < n$, where β_j is the angle between vectors defined by the boundaries of the braking range(s). Lastly, we will define λ to be the minimum angle of all braking and regular range angles.

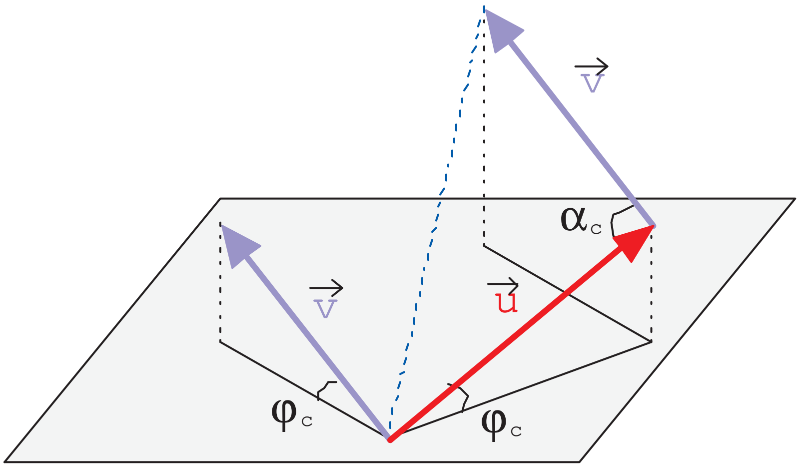

Figure 1.5: The value of α_c.

1.3 Path Types and Properties

On flat terrain, our model behaves like the weighted shortest path as in the weighted region problem of Mitchell and Papadimitriou [5] since there are no braking or impermissible ranges. That is, the path bends at edges of the terrain, obeying Snell's law of refraction. For non-flat terrains with steep slopes, the path characteristics are different. Rowe and Ross [6] show that a shortest anisotropic path can traverse a face in 4 different ways as shown in Figure 1.6. This corresponds to one of four types of face crossings which we denote as *direction types*:

1. *Regular*: Straight across at a permissible, non-braking heading obeying Snell's law along the face boundaries.

2. *Regular*: Straight across at a critical impermissibility heading to follow as close as possible to a desired direction.

3. *Switchback*: Zig-zagging along a matched pair of critical impermissibility directions.

4. *Braking*: Straight across with braking at a non-critical heading.

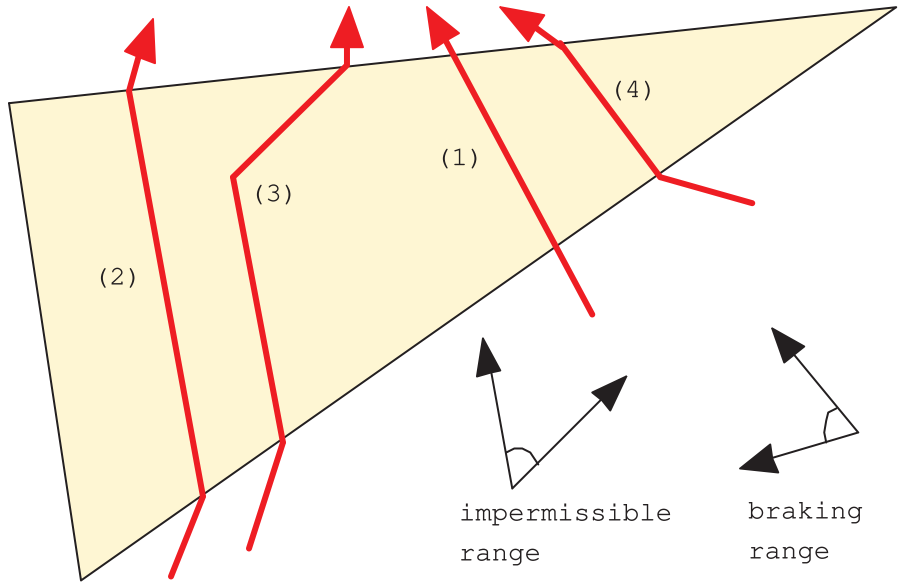

Figure 1.6: The 4 ways in which a shortest anisotropic path can cross a face.

The algorithm of Rowe and Ross [6] computes the shortest energy path for a vehicle moving in a terrain. Their algorithm computes all possible combinations of the 4 traversal types above at each edge encountered during propagation. They exhaust all posibilities through an A^* search resulting in an $O(n^n)$ algorithm in the worst case. They do however, use a set of heuristics and pruning techniques to help aleviate this large time complexity, stating that it performs much better than this pesimistic bound. Also, they assume that switchback paths are disallowed in their algorithm.

Let us examine a switchback path that passes through a face f_j. Rowe and Ross [6] show that these switchback paths are completely contained within f_j. Furthermore, they show that a switchback path consists of a chain on consecutive segments directed in the directions of a matched pair of critical impermissibility angle directions. This matched pair of angle directions, say $\vec{u}$ and $\vec{v}$, correspond to the boundaries of a single impermissibility range.

Property 1.3.1 *A switchback path between a point x of $\mathcal{P}$ and a vertex v of $\mathcal{P}$ may have an infinite number of segments.*

To understand this property, consider a switchback path from an edge of a face f_j to the vertex v opposite the edge as shown in Figure 1.7. Due to the constraint that the switchback path must lie within f_j, the number of switchbacks required to reach v is infinite. Thus, reporting a switchback path cannot be done in finite time. However, as we will see below in Claim 1.3.1,

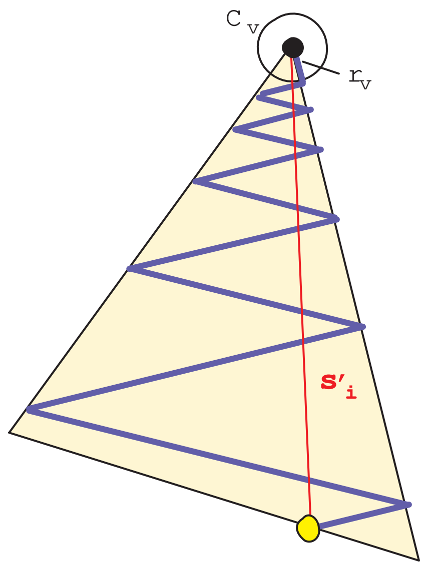

Figure 1.7: A switchback path to a vertex can have an inifinite number of segments.

the length of this path is indeed bounded. The problem can only occur when at least one of the switchback path endpoints is a vertex of $\mathcal{P}$.

In our algorithms, we will treat switchback paths as a single segment, say s_i, and assign a weight to it which incorporates the length of the switchback path itself. The following properties and claim helps bound the length of this switchback path between two given points a and b lying in the plane of f_j:

Property 1.3.2 *There exist real scalars C_1 and C_2 such that $b = a + C_1\vec{u} + C_2\vec{v}$.*

Proof: Standard vector addition property. □

Property 1.3.3 *There exist real scalars C_1 and C_2 such that $C_1|\vec{u}| + C_2|\vec{v}| \leq \frac{|\overline{ab}|}{\sin(\alpha_j/2)}$.*

Proof: Let c be the point at which $(a + C_1\vec{u})$ and $(b - C_2\vec{v})$ meet. We are sure that such a point exists because of Property 1.3.2. Thus, a, b and c form a triangle $\triangle acb$, as shown in Figure 1.8. Let $\omega = \angle cba, \psi = \angle bac$ and $\alpha_j = \angle acb$. The sine law ensures that $\sin\omega = \frac{C_1|\vec{u}|\sin\alpha_j}{|\overline{ab}|}$ and that $\sin\psi = \frac{C_2|\vec{v}|\sin\alpha_j}{|\overline{ab}|}$. Thus,

$$C_1|\vec{u}| + C_2|\vec{v}| = \left(\frac{\sin\omega}{\sin\alpha_j} + \frac{\sin\psi}{\sin\alpha_j}\right)|\overline{ab}| = \left(\frac{\sin\omega + \sin\psi}{\sin\alpha_j}\right)|\overline{ab}| \tag{1.2}$$

Now, it is clear that either $\sin\psi \geq \sin\omega$ or $\sin\psi \leq \sin\omega$. Hence, either $2\sin\psi \geq \sin\psi + \sin\omega$ or $2\sin\psi \leq \sin\psi + \sin\omega$. Therefore, one of the following is true:

$\left(\frac{2\sin\omega}{\sin\alpha_j}\right) \geq \left(\frac{\sin\omega+\sin\psi}{\sin\alpha_j}\right)$ or $\left(\frac{2\sin\psi}{\sin\alpha_j}\right) \geq \left(\frac{\sin\omega+\sin\psi}{\sin\alpha_j}\right)$

Assume that the former is true (a similar proof can be made for the later). Making a substitution into equation 1.2 results in:

$$\begin{aligned}
C_1|\vec{u}| + C_2|\vec{v}| &\leq \left(\frac{2\sin\omega}{\sin\alpha_j}\right)|\overline{ab}| \\
&\leq \left(\frac{2\sin((\pi-\alpha_j)/2)}{\sin\alpha_j}\right)|\overline{ab}| \\
&\leq \left(\frac{2\sin(\frac{\pi}{2}-\frac{\alpha_j}{2})}{\sin\alpha_j}\right)|\overline{ab}| \\
&\leq \left(\frac{2\cos(\frac{\alpha_j}{2})}{\sin\alpha_j}\right)|\overline{ab}|
\end{aligned}$$

The "half-angle formula" states that $\sin 2\alpha_j = 2\sin\alpha_j\cos\alpha_j$. We can make this substitution to obtain:

$$C_1|\vec{u}| + C_2|\vec{v}| \leq \frac{|\overline{ab}|}{\sin(\alpha_j/2)}$$

□

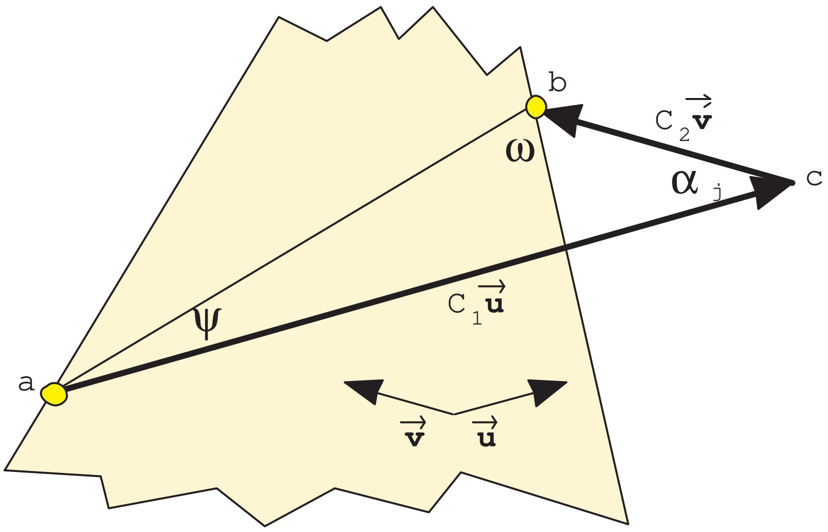

Figure 1.8: The triangle formed by extending $\vec{u}$ and $-\vec{v}$ from points a and b respectively.

Claim 1.3.1 *A switchback path between two points a and b on a face f_j which uses directions defined by $\vec{u}$ and $\vec{v}$ has length at most $\frac{|\overline{ab}|}{\sin(\alpha_j/2)}$.*

Proof: In the case of a two-link switchback path, the claim is true due to Property 1.3.3. Since switchback paths for a given impermissibility range travel in at most two non-parallel directions, the path is essentially using a manhatten metric defined by the two non-parallel vectors. Hence, all switchback paths for a given impermissibility range between a and b have equal length. From Property 1.3.3, this length is at most $\frac{|\overline{ab}|}{\sin(\alpha_j/2)}|\overline{ab}|$. $\square$

Some further definitions are required. Define h_v to be the minimum distance from v to the boundary of the union of its incident faces. Let $r_v = \epsilon h_v$ for some $\epsilon > 0$. Let r be the minimum r_v over all v.

1.4 A Simple Approach to Approximation

Our aim is to improve the large running time of Rowe and Ross [6] through approximation. Our first approach is similar to the *Fixed Scheme* of our Euclidean and weighted cost shortest path approximation techniques [4]. Recall that this scheme adds m Steiner points along each edge of the terrain and then connects the Steiner points of each face with a complete graph. The global graph is then searched using Dijkstra's algorithm to obtain the approximation. This approach cannot be directly applied to the anisotropic shortest path problem since it may produce edges that are immpermissible for travel. The problem does not lie in the placement of Steiner points, but rather lies in the direction and weights of the edges connecting them. The simple approach here is to also build a graph; the main difference in this graph lies in the weights that are placed on the graph edges, which is based on direction.

1.4.1 Building the Graph

For each face f_j of $\mathcal{P}$, we build a graph G_j. We begin by placing m equally spaced Steiner points along each edge of f_j, for some positive integer m. The vertices of G_i are the vertices of f_j as well as these Steiner points. Connect p and q with 2 directed edges $\overrightarrow{pq}$ and $\overrightarrow{qp}$, where p and q are Steiner points on different edges of f_j. Connect adjacent Steiner points on the same edge of f_j by two oppositely directed edges as well. Lastly, connect each vertex v of f_j to all Steiner points on the edge of f_j opposite to v with two oppositely directed edges.

We now assign weights to the edges of G_j. For each edge e of G_j that is directed in a heading that is non-braking and non-impermissible, its weight is set to be $w_j|e|$. For edges whose direction falls within the braking range, they are given weight equal to $-\sin\varphi_i|e|$. This essentially assigns a weight on the edge equal to the change in elevation. Note again that φ_i is a negative angle in this case and the weight will therefore be positive. For edges representing impermissible headings, they are assigned a weight corresponding to the length of a permissible switchback path between their endpoints. From Claim 1.3.1 we know that this length is at most $\frac{|e|}{\sin\frac{\alpha_j}{2}}$. However, this is an upper bound on the length. In fact, we can assign the exact length of the path as stated in Property 1.3.3. This length is $\left(\frac{\sin\omega+\sin\psi}{\sin\alpha_j}\right)|e|$, where ω and ψ are defined as shown in Figure 1.8. Hence the weight of e is set to $w_j\left(\frac{\sin\omega+\sin\psi}{\sin\alpha_j}\right)|e|$ In our analysis, however, we will be bounding these switchback paths with the cost of $\frac{w_j|e|}{\sin\frac{\alpha_j}{2}}$. This concludes our construction of G_j. A global graph G is then constructed as the union of all $G_j, 1 \le j \le n$.

Claim 1.4.1 *Each edge $e \in G$ represents a path on $\mathcal{P}$ that has bounded cost.*

Proof: Regular and braking edges of G clearly have bounded cost since their lengths are finite and they correspond to a single-segment on $\mathcal{P}$. Claim 1.3.1 ensures that Switchback edges of G represent paths that have bounded length and therefore, bounded cost. Note that we are not saying anything about the number of segments in the switchback paths since Property 1.3.1 indicates this may be unbounded. □

1.4.2 Constructing an Approximated Path

Given a shortest anisotropic path $\Pi(s,t)$ on $\mathcal{P}$, we describe here a particular path $\Pi'(s,t)$ in G which has a bounded cost with respect to $\Pi(s,t)$. Some of the segments of $\Pi'(s,t)$ may be "flagged" as *switchback* indicating that when the approximated path is to be reported, then these segments are to be replaced by a switchback path between their endpoints. A distinction is therefore required between the path in G and the path that will be reported. The reported path will be denoted as $\Pi''(s,t)$. We denote the number of segments of $\Pi(s,t), \Pi'(s,t)$ and $\Pi''(s,t)$ as k, k' and k'', respectively.

We consider the case in which $\Pi'(s,t)$ has segments that pass through the same faces (in the same order) as those of $\Pi(s,t)$. We will consider this path in our analysis of the approximation factor, although it may be the case that the running of Dijkstra's algorithm produces a better path.

Consider a segment s_i of $\Pi(s,t)$ passing through face f_j, where $0 < i < k$. Let p and q be the vertices of G_j corresponding to Steiner points (or vertices) on edges of f_j that are closest (Euclidean distance) to the endpoints of s_i. If $p \neq q$ then let $s'_i = \overline{pq}$ be the edge of $\Pi'(s,t)$ that approximates s_i. If $p = q$ then let $s'_i = \emptyset$. Note that this situation only occurs when s_i crosses a face close to a vertex or when s_i travels very briefly along an edge of $\mathcal{P}$ (see Figure 1.9). Once this is done for each segment of $\Pi(s,t)$, we remove all of the $\emptyset$ edges. Note also that if two or more consecutive edges are collinear, then these edges are merged as one. The resulting sequence of edges is $\Pi'(s,t)$. This construction ensures that $k' \leq k$.

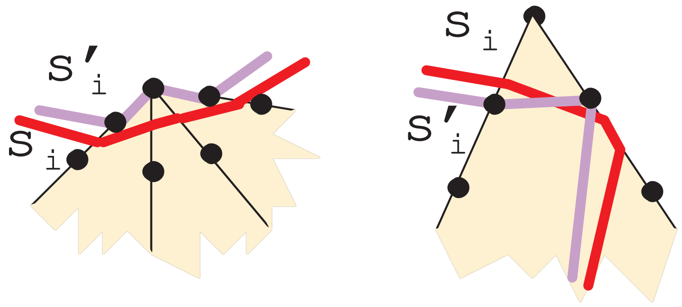

Figure 1.9: When a segment s_i of $\Pi(s,t)$ is approximated near a vertex or briefly along an edge of $\mathcal{P}$, there may be no corresponding segment in $\Pi'(s,t)$.

Claim 1.4.2 $\Pi'(s,t)$ *is connected.*

Proof: In order to show connectivity of $\Pi'(s,t)$ we just need to show that adjacent edges s'_i and s'_{i+1} are connected, where $0 < i \leq k'$. Now s'_i and s'_{i+1} have been chosen as passing through the same segments as s_i and s_{i+1}. Hence s_i and s_{i+1} share an endpoint, say x. Now s'_i and s'_{i+1} also share an endpoint which is the closer Steiner point to x. Thus, s'_i and s'_{i+1} are connected. In the case where this shared endpoint is a vertex of $\mathcal{P}$, we can provide an iterative analysis to show for some constants c_1 and c_2 that s'_{i-c_1} and s'_{i+c_2} share the vertex as an endpoint. Also, a similar analysis can be made for the second case of Figure 1.9 in which the path travels briefly along the edge. Hence $\Pi'(s,t)$ is connected. □

If we are merely interested in reporting the cost of the approximated path, then we only need to report $\|\Pi'(s,t)\|$. However, if the path itself is required, it cannot necessarily be reported in $O(k')$ time since switchback segments of $\Pi'(s,t)$ may represent a large chain of segments whose number of links may be infinite and which depends on geometric parameters such as α and θ. We will therefore construct a path $\Pi''(s,t)$ from $\Pi'(s,t)$ in which all of these *switchback* edges are expanded to a finite number of actual segments on $\mathcal{P}$. Thus, it is always the case that $k'' \geq k'$.

To begin, each regular and braking edge s'_i of $\Pi'(s,t)$ has an equivalent (i.e. identical) segment s''_i in $\Pi'(s,t)$. For each switchback path s'_i of $\Pi'(s,t)$, we will construct a finite-segment switchback path z''_i in $\Pi''(s,t)$. To form $\Pi''(s,t)$ we concatenate all s''_i and z''_i in the order from $i=1$ to $i=k'$. Recall that $\|s'_i\|$ encapsulates the length of a two-link switchback path. We cannot merely assign this two-link path as $z''_i = \{s''_j, s''_{j+1}\}$ since it may not lie completely within a single face. We can however "adjust" this two-link path (by creating more links) such that the newly adjusted path lies within the face (see Figure 1.10). We will set z''_i to be this adjusted path. Claim 1.3.1 ensures that $\|z''_i\| = \|s'_i\|$.

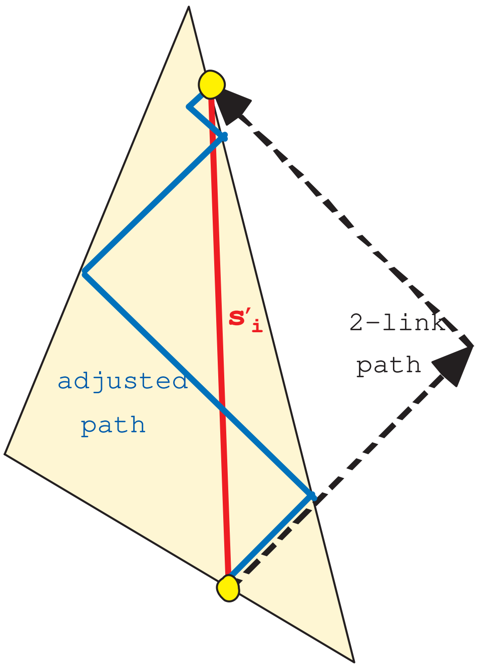

Figure 1.10: Adjusting a 2-link path such that it lies within the face.

This creation of z_i'', however, will cause a significant problem in the case where at least one of the endpoints of s_i' is a vertex, say v. The problem is as depicted in Property 1.3.1, in which z_i'' has an infinite number of segments. To handle this problem, we merely limit z_i'' to contain only one switchback segment that intersects C_v (i.e. the sphere around v). To do this, we can iteratively append consecutive switchback segments to z_i'' until we get one that intersects C_v. z_i'' is then completed with a segment from the last of these switchback segments to v. Although, this last link will be in an impermissible direction, we can make it arbitrarily small in length and so this should be feasible in practice.

A further problem is that of travelling on an edge in an impermissible direction. Let s_i' be a segment of our approximation that lies along an edge e of $\mathcal{P}$. If s_i' is directed in an impermissible direction, then it is clearly impossible to zig-zag along e. In this case, we construct z_i'' as before, but such that the segments of z_i'' all lie in one of the faces adjacent to e (i.e. the face with minimum path cost).

Claim 1.4.3 *If a valid path $\Pi(s,t)$ exists between two vertices s and t of $\mathcal{P}$ then there exists a path $\Pi'(s,t)$ in G and hence a valid path $\Pi''(s,t)$ on $\mathcal{P}$.*

Proof: Since $\Pi(s,t)$ is valid, then by definition, it's segments must all be in permissible directions. Each segment s' of $\Pi'(s,t)$ corresponds to a segment s of $\Pi(s,t)$ that passes through the same face. By definition, the faces through which $\Pi(s,t)$ passes cannot be isotropic obstacles and so the faces through which $\Pi'(s,t)$ passes cannot be isotropic obstacles as well. Therefore, since s and t are vertices of G then there exists a path in G. Now since each edge of G represents either a valid edge or a switchback path of $\Pi''(s,t)$, then $\Pi''(s,t)$ must also exist. □

1.4.3 Computing a Bound on the Approximation

In order to determine the accuracy of $\Pi'(s,t)$, we apply a similar segment-by-segment analysis as with the weighted scheme of Lanthier et. al. [4]. The analysis becomes slightly more complex due to the special cases of braking and switchbacks. That is, we must consider the situation in which a shortest path segment is approximated by a segment that has a different type (e.g., s_i is a braking segment and s_i' is a switchback path). Note that during the analysis, we do not need to consider the number of segments in the switchback paths, only the bound on the length of such paths. The bound of $\|\Pi'(s,t)\|$ will therefore apply to $\|\Pi''(s,t)\|$. Throughout the analysis, we will make use of the Lemma of Lanthier et. al. [4] which states that

$$|s_i'| \le |s_i| + \frac{|L|}{m+1}. \tag{1.3}$$

where L is the longest edge of $\mathcal{P}$ and m is the number of Steiner points placed on each edge of $\mathcal{P}$.

Given a segment s_i (or switchback path z_i) passing through face f_j, we will bound the cost of s_i'. We will consider the nine possible cases which correspond to iterating through the three types of direction types for s_i and s_i' each.

Claim 1.4.4 *If both s_i and s_i' are regular, then $\|s_i'\| \le \|s_i\| + \frac{w_j|L|}{m+1}$*

Proof: Multiplying equation (1.3) by w_j, we obtain $w_j|s_i'| \le w_j|s_i| + w_j\frac{|L|}{m+1}$. Substituting the weighted cost for s_i and s_i', we realize that this is none other than $\|s_i'\| \le \|s_i\| + \frac{w_j|L|}{m+1}$.

$\square$

Claim 1.4.5 *If s_i is regular and s'_i is braking, then* $\|s'_i\| \leq -\sin\varphi'_i\left(\frac{\|s_i\|}{w_j} + \frac{|L|}{m+1}\right)$.

Proof: From our weight metric we obtain $\|s_i\| = w_j|s_i|$ and $\|s'_i\| = -\sin\varphi'_i|s'_i|$. Substituting equation (1.3) for $|s'_i|$ results in:

$$\begin{aligned}
\|s'_i\| &= -\sin\varphi'_i|s'_i| \\
&\leq -\sin\varphi'_i(|s_i| + \frac{|L|}{m+1}) \\
&= -\sin\varphi'_i(\frac{1}{w_j}\|s_i\| + \frac{|L|}{m+1}).
\end{aligned}$$

$\square$

Claim 1.4.6 *If s_i is regular and s'_i is switchback, then* $\|s'_i\| \leq \frac{1}{\sin\frac{\alpha_j}{2}}\left(\|s_i\| + \frac{w_j|L|}{m+1}\right)$.

Proof: From our weight metric we have $\|s'_i\| \leq \frac{w_j}{\sin\frac{\alpha_j}{2}}|s'_i|$. Substituting equation (1.3) for $|s'_i|$ results in:

$$\begin{aligned}
\|s'_i\| &\leq \frac{w_j}{\sin\frac{\alpha_j}{2}}\left(|s_i| + \frac{|L|}{m+1}\right) \\
&= \frac{w_j}{\sin\frac{\alpha_j}{2}}\left(\frac{\|s_i\|}{w_j} + \frac{|L|}{m+1}\right) \\
&= \frac{1}{\sin\frac{\alpha_j}{2}}\left(\|s_i\| + \frac{w_j|L|}{m+1}\right).
\end{aligned}$$

$\square$

Claim 1.4.7 *If s_i is braking and s'_i is regular, then* $\|s'_i\| \leq \frac{w_j}{-\sin\varphi_i}\|s_i\| + \frac{w_j|L|}{m+1}$.

Proof: From our weight metric we obtain $\|s'_i\| = w_j|s'_i|$ and $\|s_i\| = -\sin\varphi_i|s_i|$. Substituting the results of equation (1.3) results in:

$$\begin{aligned}
\|s'_i\| &= w_j|s'_i| \\
&\leq w_j(|s_i| + \frac{|L|}{m+1}) \\
&= w_j(\frac{\|s_i\|}{-\sin\varphi_i} + \frac{|L|}{m+1}) \\
&= \frac{w_j}{-\sin\varphi_i}\|s_i\| + \frac{w_j|L|}{m+1}.
\end{aligned}$$

$\square$

Claim 1.4.8 *If both s_i and s'_i are braking, then* $\|s'_i\| \leq \|s_i\| + \frac{|L|}{m+1}$.

Proof: From our weight metric we obtain $\|s_i'\| = -\sin\varphi_i'|s_i'|$ and $\|s_i\| = -\sin\varphi_i|s_i|$. Here $\|s_i'\|$ represents the change in height between its endpoints; similarly for $\|s_i\|$. The difference in height between $\|s_i'\|$ and $\|s_i\|$ can be at most $\frac{|L|}{m+1}$ (which would occur if the face was vertical). Therefore, $\|s_i'\| \leq \|s_i\| + \frac{|L|}{m+1}$. □

Claim 1.4.9 *If s_i is braking and s_i' is switchback, then $\|s_i'\| \leq \frac{w_j}{\sin\frac{\alpha_j}{2}}\left(\frac{\|s_i\|}{-\sin\varphi_i} + \frac{|L|}{m+1}\right)$.*

Proof: From our weight metric we obtain $\|s_i\| = -\sin\varphi_i|s_i|$ and $\|s_i'\| \leq \frac{w_j}{\sin\frac{\alpha_j}{2}}|s_i'|$. Substituting this into equation (1.3) results in:

$$\begin{aligned}
\|s_i'\| &\leq \frac{w_j}{\sin\frac{\alpha_j}{2}}\left(|s_i| + \frac{|L|}{m+1}\right) \\
&= \frac{w_j}{\sin\frac{\alpha_j}{2}}\left(\frac{1}{-\sin\varphi_i}\|s_i\| + \frac{|L|}{m+1}\right).
\end{aligned}$$

□

Claim 1.4.10 *If s_i is switchback and s_i' is regular, then $\|s_i'\| \leq \|s_i\| + \frac{w_j|L|}{m+1}$.*

Proof: From our weight metric we are ensured that $\|s_i'\| = w_j|s_i'|$. Now since s_i is switchback, then $\|s_i\| = w_j|z_i| > w_j|s_i|$. Using equation (1.3) we obtain:

$$\begin{aligned}
\|s_i'\| &= w_j|s_i'| \\
&\leq w_j(|s_i| + \frac{|L|}{m+1}) \\
&\leq w_j\left(\frac{\|s_i\|}{w_j} + \frac{|L|}{m+1}\right) \\
&= \|s_i\| + \frac{w_j|L|}{m+1}.
\end{aligned}$$

□

Claim 1.4.11 *If s_i is switchback and s_i' is braking, then $\|s_i'\| \leq -\sin\varphi_i'\left(\frac{\|s_i\|}{w_j} + \frac{|L|}{m+1}\right)$.*

Proof: From our weight metric we have $\|s_i'\| = -\sin\varphi_i'|s_i'|$. Now since s_i is switchback, then $\|s_i\| = w_j|z_i| > w_j|s_i|$. Using equation (1.3) we obtain:

$$\begin{aligned}
\|s_i'\| &= -\sin\varphi_i'|s_i'| \\
&\leq -\sin\varphi_i'(|s_i| + \frac{|L|}{m+1}) \\
&\leq -\sin\varphi_i'\left(\frac{\|s_i\|}{w_j} + \frac{|L|}{m+1}\right).
\end{aligned}$$

□

Claim 1.4.12 *If both s_i and s'_i are switchback, then* $\|s'_i\| \leq \frac{1}{\sin\frac{\alpha_j}{2}}\left(\|s_i\| + \frac{w_j|L|}{(m+1)}\right)$.

Proof: From our weight metric we have $\|s'_i\| \leq \frac{w_j}{\sin\frac{\alpha_j}{2}}|s'_i|$. Now since s_i is switchback, then $\|s_i\| = w_j|z_i| > w_j|s_i|$. Substituting in equation (1.3) results in:

$$\begin{aligned}\|s'_i\| &\leq \frac{w_j}{\sin\frac{\alpha_j}{2}}\left(|s_i| + \frac{|L|}{m+1}\right)\\ &\leq \frac{w_j}{\sin\frac{\alpha_j}{2}}\left(\frac{\|s_i\|}{w_j} + \frac{|L|}{m+1}\right)\\ &= \frac{1}{\sin\frac{\alpha_j}{2}}\left(\|s_i\| + \frac{w_j|L|}{(m+1)}\right).\end{aligned}$$

□

Table 1.4.3 gathers the results of the claims just presented. It shows the bounds for each type of segment s'_i as compared to the type of s_i. As can be seen, the bound may be very bad in the worst case.

$s_i \ \backslash \ s'_i$	Regular	Braking	Switchback
Regular	$\|s_i\| + \frac{w_j\|L\|}{m+1}$	$-\sin\varphi'_i(\frac{\|s_i\|}{w_j} + \frac{\|L\|}{m+1})$	$\frac{1}{\sin\frac{\alpha_j}{2}}\left(\|s_i\| + \frac{w_j\|L\|}{m+1}\right)$
Braking	$\frac{w_j}{-\sin\varphi_i}\|s_i\| + \frac{w_j\|L\|}{m+1}$	$\|s_i\| + \frac{\|L\|}{m+1}$	$\frac{w_j}{\sin\frac{\alpha_j}{2}}\left(\frac{\|s_i\|}{-\sin\varphi_i} + \frac{\|L\|}{m+1}\right)$
Switchback	$\|s_i\| + \frac{w_j\|L\|}{m+1}$	$-\sin\varphi'_i\left(\frac{\|s_i\|}{w_j} + \frac{\|L\|}{m+1}\right)$	$\frac{1}{\sin\frac{\alpha_j}{2}}\left(\|s_i\| + \frac{w_j\|L\|}{(m+1)}\right)$

Table 1.2: The maximum cost of the approximated segment s'_i w.r.t. the actual shortest path segment cost $\|s_i\|$. Here $w_j = \mu_j \cos\phi_j$.

Lemma 1.4.1 *Given two vertices s and t of G, there exists a path $\Pi'(s,t)$ in G such that* $\|\Pi'(s,t)\| \leq \frac{1}{\sin\frac{\alpha}{2}}\|\Pi(s,t)\| + \frac{W|L|k}{(m+1)\sin\frac{\alpha}{2}}$, *where k is the number of segments of $\Pi(s,t)$.*

Proof: Let $\Pi(s,t) = \{s_1, s_2, \cdots, s_k\}$. For each $s_j \in \Pi(s,t)$, it follows from the results in Table 1.4.3 that there exists an edge $s'_j \in G$ that approximates s_j. Let $\Pi'(s,t) = \{s'_1, s'_2, \cdots, s'_k\} \in G$. Observe that due to the construction, $\Pi'(s,t)$ is a connected path. It is not difficult to see that the worst case approximation from Table 1.4.3 is that of $\|s'_i\| \leq \frac{1}{\sin\frac{\alpha_j}{2}}\|s_i\| + \frac{w_j|L|}{(m+1)\sin\frac{\alpha_j}{2}}$. To see this, we make use of Property 1.2.1 which states that $-\sin\varphi_i$ is at least w_j. By applying this worst case approximation to all segments of $\Pi'(s,t)$ we have:

$$\sum_{i=1}^{k}\|s_i'\| \;\leq\; \sum_{i=1}^{k}\frac{1}{\sin\frac{\alpha_j}{2}}\left(\|s_i\|+\frac{w_j|L|}{m+1}\right).$$

We can now put an upper bound on w_j and a lower bound on α_j:

$$\begin{aligned}\|\Pi'(s,t)\| &\leq \sum_{i=1}^{k}\frac{1}{\sin\frac{\alpha}{2}}\left(\|s_i\|+\frac{W|L|}{m+1}\right)\\ &\leq \frac{1}{\sin\frac{\alpha}{2}}\|\Pi(s,t)\|+\frac{W|L|k}{(m+1)\sin\frac{\alpha}{2}}.\end{aligned}$$

□

Theorem 1.4.1 *We can compute an approximation $\Pi'(s,t)$ of the weighted shortest anisotropic path $\Pi(s,t)$ between two vertices s and t of G such that $\|\Pi'(s,t)\| \leq \frac{1}{\sin\frac{\alpha}{2}}(\|\Pi(s,t)\|+W|L|)$. Moreover, we can compute this path in $O(nk\log nk+nk^2)$ time, where k is the number of segments of $\|\Pi(s,t)\|$.*

Proof: In Lemma 1.4.1 we have shown that there is a path $\Pi'(s,t)$ in G that approximates a shortest path $\Pi(s,t)$ on P. We use Dijktra's algorithm to compute a shortest path between the vertices corresponding to s and t in G. This will result in a path in G that has either the same cost as $\Pi'(s,t)$ or even less. Since any path in G can be mapped to a path on P, we obtain an approximate path on P. In Lemma 1.4.1, set $m = k-1$ to obtain the specified accuracy. Now we analyze the time complexity of the algorithm. Each edge of $\mathcal{P}$ contributes $O(m)$ graph vertices and each face contributes $O(m^2)$ graph edges. Dijkstra's algorithm is then applied which runs in $O(nk\log nk+nk^2)$ time. □

We have just given a bound on the accuracy of the approximated path produced using this simple approach. The approximated path accuracy depends upon geometric parameters of the terrain: L, α, and W. Since the value of α can be arbitrarily small, the path accuracy can be arbitrarily bad. However, in most traversable terrain, there is a limit on reasonable values of α which allows the path accuracy to be reasonably bounded in practice. The problem with this method is that k is unknown. It remains an open question as to how big k may be. In the weighted shortest path problem, it has been shown that k can be $\theta(n^2)$, however this does not apply to the anisotropic shortest path problem since $\|\Pi(s,t)\|$ can pass through a face more than $O(n)$ times. Figure 1.11 shows an example of a case in which there are $\Omega(n)$ segments of $\|\Pi(s,t)\|$ that cross a face. In the example, the number of times a face is crossed depends on some function of n and α.

During the analysis, we made the assumption that each segment of $\Pi(s,t)$ was approximated in the worst possible manner. That is, we assumed that all segments of $\Pi'(s,t)$ were switchback. Clearly this is very unlikely since the switchback paths are more expensive than the regular and braking segments. Therefore, we can easily conclude that the stated path accuracy is not a "tight" bound for the average case. It is very likely that the bound will be much better in practice. Due to its simplicty it is likely that this algorithm is of practical value and is likely to produce accuracte paths with only a few Steiner points added per edge (as in [4]).

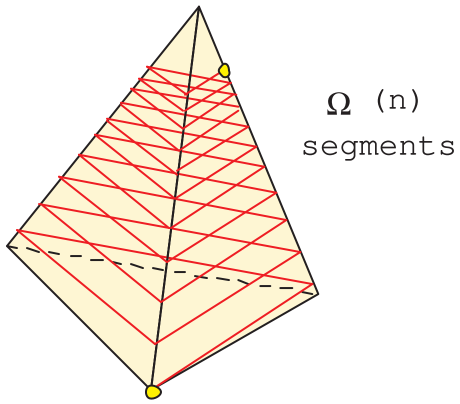

Figure 1.11: Example in which $\Omega(n)$ segments of $\|\Pi(s,t)\|$ cross a given face.

1.5 An ϵ-Approximation

In this section, we present an algorithm that produces an approximation with improved worst case path accuracy. The basic notion of the algorithm is the same, and differs mainly in the number and placement of Steiner points on the edges of $\mathcal{P}$.

From the results in Table 1.4.3, it is easily seen that in order to improve the path accuracy, we must ensure that segments of $\Pi(s,t)$ are approximated with segments of $\Pi'(s,t)$ that have equal or better weight. For example, braking segments of $\Pi(s,t)$ must be approximated with braking segments of $\Pi'(s,t)$. This is one of the main objectives of this improved scheme. In addition, this improvement will ensure that each segment s_i of $\Pi(s,t)$ is approximated with a corresponding segment s_i' of $\Pi'(s,t)$ such that $\|s_i'\| \leq (1+f(\epsilon))\|s_i\|$, where $f(\epsilon)$ is some function which depends on geometric parameters of $\mathcal{P}$, but is independent of n. This will ensure that $\Pi'(s,t)$ is an ϵ-approximation of $\Pi(s,t)$. This improved scheme also adds Steiner points to edges of $\mathcal{P}$ and then builds a graph from which the approximation will be computed. We will show that the main difference in the results of this algorithm and that of [1] and [2] is the number of Steiner points that are used and in the size of each r_v.

To begin, we require a few definitions. Define h_v to be the minimum distance from v to the boundary of the union of its incident faces. Define a polygonal cap C_v, called a *sphere*, around v, as follows. Let $r_v = \epsilon h_v$ for some $\epsilon > 0$. Let r be the minimum r_v over all v. Let $\triangle vuw$ be a face incident to v. Let u' (w') be at the distance of r_v from v on $\overline{vu}$ ($\overline{vw}$). This defines a triangular subface $\triangle vu'w'$ of $\triangle vuw$. The sphere C_v around v consists of all such subfaces incident at v.

Property 1.5.1 *The distance between any two spheres C_{v_a} and C_{v_b} is at least $(1-2\epsilon)h_{v_a}$.*

1.5.1 Building the Graph

We begin by constructing a graph G_j for each face f_j of $\mathcal{P}$ by adding Steiner points along edges of f_j in three stages. In the first stage, we add enough Steiner points to ensure that the distance between adjacent Steiner points on an edge is sufficiently small. In essence, we will make this distance small enough to ensure that it is at most $f(\epsilon)$ times the length of a shortest path segment which passes through it, for some function $f(\epsilon)$ which is independent of n. For each vertex v of face f_j we do the following: Let e_q and e_p be the edges of f_j incident to v. First, place Steiner points on edges e_q and e_p at distance r_v from v; call them q_1 and p_1, respectively. By definition, $|\overline{vq_1}| = |\overline{vp_1}| = r_v$. Define $\delta = (1 + \epsilon \sin \theta_v)$ if $\theta_v < \frac{\pi}{2}$, otherwise $\delta = (1 + \epsilon)$. We now add Steiner points $q_2, q_3, ..., q_{\iota_q - 1}$ along e_q such that $|\overline{vq_j}| = r_v \delta^{j-1}$ where $\iota_q = \log_\delta(|e_q|/r_v)$. Similarly, add Steiner points $p_2, p_3, ..., p_{\iota_p - 1}$ along e_p, where $\iota_p = \log_\delta(|e_p|/r_v)$.

Claim 1.5.1 *$|\overline{q_i q_{i+1}}| = \epsilon \cdot dist(q_i, e_p)$ and $|\overline{p_j p_{j+1}}| = \epsilon \cdot dist(p_j, e_q)$ where $0 < i < \iota_q$ and $0 < j < \iota_p$.*

Proof: The proof is shown for $|\overline{q_i q_{i+1}}|$ (a symmetrical proof can be constructed for $|\overline{p_j p_{j+1}}|$). We can manipulate $|\overline{q_i q_{i+1}}|$ as follows:

$$|\overline{q_i q_{i+1}}| = |\overline{vq_{i+1}}| - |\overline{vq_i}| = r_v \delta^i - r_v \delta^{i-1} = r_v \delta^{i-1}(\delta - 1) = |\overline{vq_i}|(\delta - 1)$$

If $\theta_v < \frac{\pi}{2}$, then by definition, $\delta = (1 + \sin \theta_v \epsilon)$, and so

$$|\overline{q_i q_{i+1}}| = |\overline{vq_i}|(1 + \sin \theta_v \epsilon - 1) = \sin \theta_v \epsilon |\overline{vq_i}|$$

Since $\mathrm{dist}(q_i, e_p) = \sin \theta_v |\overline{vq_i}|$ by definition, then $|\overline{q_i q_{i+1}}| = \epsilon \cdot \mathrm{dist}(q_i, e_p)$.

Now if $\theta_v \geq \frac{\pi}{2}$, then by definition, $\delta = (1 + \epsilon)$, and so

$$|\overline{q_i q_{i+1}}| = |\overline{vq_i}|(1 + \epsilon - 1) = \epsilon |\overline{vq_i}|$$

Since $\mathrm{dist}(q_i, e_p) = |\overline{vq_i}|$ by definition when $\theta_v \geq \frac{\pi}{2}$, then $|\overline{q_i q_{i+1}}| = \epsilon \cdot \mathrm{dist}(q_i, e_p)$. □

Since this construction is made for each vertex of a face f_j, there will be two overlapping sets of Steiner points on each edge of f_j. To eliminate this overlap, we reduce the number of Steiner points on each edge. Given an edge e and its two sets of Steiner points originating from the endpoints of e, we determine the point on e where the interval sizes from each set are equal and eliminate all larger intervals. Intuitively, intervals are eliminated from one set if there are smaller intervals in the other set that overlap with it. Figure 1.12 depicts the results of applying this technique to a face.

Now we add a second stage of Steiner points which are required to ensure that there exists an approximation segment with the same direction type as a shortest path segment which passes between the same Steiner points. Recall that our model of computation allows for eight direction ranges (three impermissible, one braking and four regular) per face as shown in Figure 1.3. We will add a set of Steiner points to f_j corresponding to the braking range and the (up to four) regular ranges. We give here a description of how to add the Steiner points corresponding to the braking range; the Steiner point sets for the regular ranges are constructed in the same manner. Let $\vec{u}$ and $\vec{v}$ be the critical angle directions for the range on the plane of f_j. Consider now each vertex v of f_j and apply the following algorithm twice (once as is and then again where $\vec{u}$ and $\vec{v}$ are swapped):

LET $q = v$.
WHILE (q does not lie within C_{v_i} of f_j, where $v_i \neq v$) DO {
    LET x_q be a ray from q in direction $\vec{u}$.
    IF (x_q intersects an edge e of f_j) THEN {
        $p =$ intersection point of x_q and e.
        Add p as a Steiner point on e.
        LET x_p be a ray from p in direction $-\vec{v}$.
        IF (x_p does not intersect an edge e of f_j) THEN STOP

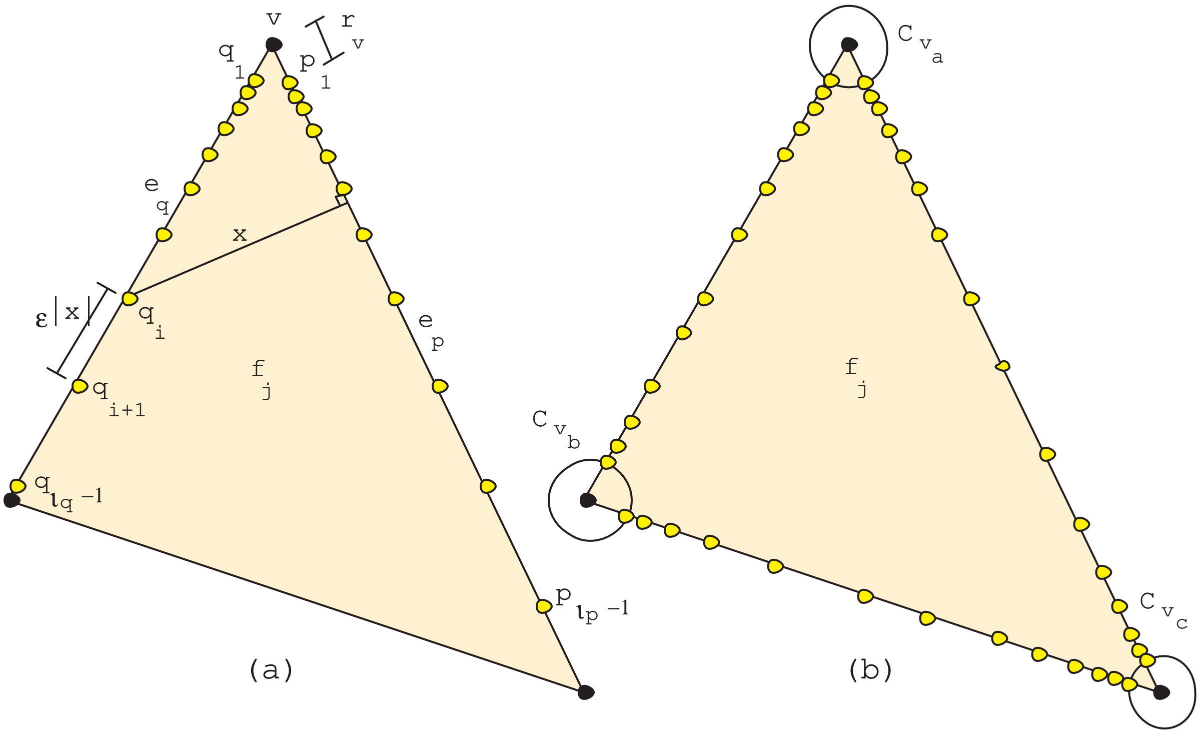

Figure 1.12: a) Placement of Steiner points on the edges of f_j that are incident to vertex v. b) Results of merging Steiner points along edges of f_j.

ELSE {
    q = intersection point of x_p with e.
    Add q as a Steiner point on e.
  }
 }
}

Figure 1.13 shows how these Steiner points are added using this algorithm. Note that when applying this stage to the adjacent faces of f_j, some additional Steiner points will be added to the edges of f_j. When creating the graph for an adjacent face f_{j+1}, each edge of f_j may also gain a set of Steiner points due to this second stage construction. Hence, each edge may have two such sets of Steiner points. The first and second stage of Steiner points along with the vertices of f_j become vertices of G_j. Connect a pair of vertices in G_j by two oppositely directed edges iff 1) they represent Steiner points lying on different edges of f_j or 2) they represent adjacent Steiner points lying on the same edge of f_j. In addition, for each vertex of G_j which corresponds to a vertex, say v, of f_j, connect it with two oppositly directed edges to 1) all vertices of G_j that represent Steiner points lying on the edge opposite to v, and 2) the two vertices of G_j corresponding to the two closest Steiner points that lie on the two incident edges of v.

In the final stage, we expand G_j by placing additional vertices (i.e., Steiner points) within at least one of the spheres around a vertex of f_j. Let q be a Steiner point (or vertex of f_j) on edge e_q

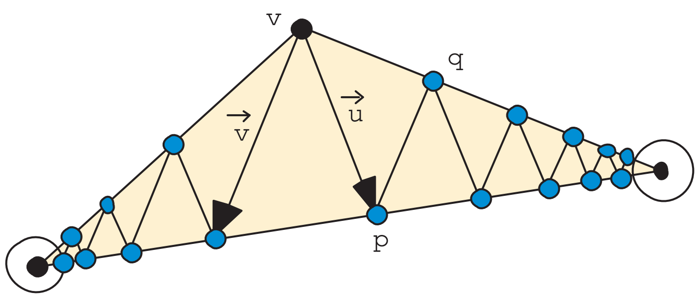

Figure 1.13: Adding Steiner points to a face corresponding to a braking range.

of f_j which was added during the first or second stage of Steiner placement (including those from adjacent faces as well). Extend rays from q in the directions of $\vec{u}$ and $\vec{v}$. For each ray, if it intersects an edge $e_p \neq e_q$ of f_j at some point x within some C_v of vertex v of f_j then add a Steiner point at x. Add x as a vertex of G_j and add edge $\overrightarrow{qx}$ to G_j. Also add edge $\overrightarrow{xv}$ to G_j. Now extend rays from q in the directions of $-\vec{u}$ and $-\vec{v}$. For each ray, if it intersects an edge $e_p \neq e_q$ of f_j at some point x within a distance of r_v of a vertex v of f_j then add a Steiner point at x. Add x as a vertex of G_j and add edge $\overrightarrow{xq}$ to G_j. Also add edge $\overrightarrow{vx}$ to G_j. Figure 1.14 shows how these new Steiner points are added near a vertex v.

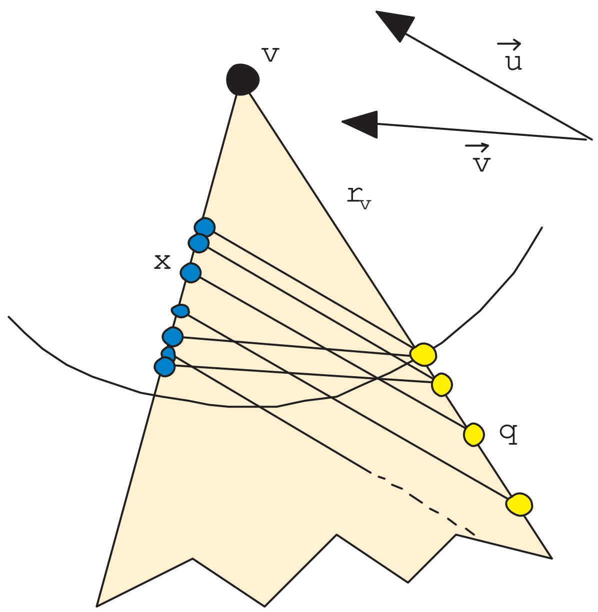

Figure 1.14: Adding Steiner points to a face within a sphere around vertex v.

Let q_a and q_{a+1} be two adjacent Steiner points added on an edge within a sphere C_v as just mentionned. Let p_b and p_{b+1} be the Steiner points that generated q_a and q_{a+1}, respectively. If

$|\overline{q_a q_{a+1}}| > r_v(\delta - 1)$ then we add additional evenly spaced Steiner points between q_a and q_{a+1}. We add only enough Steiner points to ensure that the distance between two adjacent points is at most $r_v(\delta - 1)$. Once again, connect each of these new Steiner points, say p to v with two oppositely directed edges. Also, connect p to p_b and p_{b+1} with two oppositely directed edges each. Keep in mind that although we just described the addition of these Steiner points with respect to the two critical directions $\vec{u}$ and $\vec{v}$ for the braking range, we must also add similar sets of Steiner points for the regular ranges.

We are done adding vertices and edges to G_j. We must now assign appropriate weights to the edges. For each edge $\overrightarrow{ab}$ of G_j, we set its weight as follows:

1. If $\overrightarrow{ab}$ is regular then its weight is set to $w_j|\overline{ab}|$.
2. If $\overrightarrow{ab}$ is braking then its weight is set to $-\sin\theta_i|\overline{ab}|$ where θ_i is the declination angle of $\overrightarrow{ab}$.
3. If $\overrightarrow{ab}$ is switchback then its weight is set to $\frac{w_j}{\sin\frac{\alpha}{2}}|\overline{ab}|$.

This completes the construction of G_j. A graph G is defined to be the union $G_1 \cup G_2 \cup ... G_n$. The following claims can be made as done in [1] and [2].

Claim 1.5.2 *G is connected.*

Claim 1.5.3 *At most $m = O(\log_\delta(|L|/r) + \log_{\mathcal{F}}(r/|L|))$ Steiner points are added to each edge of f_j, where $\mathcal{F} = \frac{1+\cos(\theta+\lambda)}{1+\cos(\theta-\lambda)}$.*

Proof: The number of Steiner points added in stage 1 of the algorithm has been proven to be $O(\log_\delta(|L|/r))$ in [2]. The number of Steiner points added in stage 3 of the algorithm is of the same order as that which was added during stage 2. We therefore need to consider the Steiner points added in stage 2 of the algorithm. Let $\vec{u}$ and $\vec{v}$ be the two critical angle vectors corresponding to either the braking range or one of the regular ranges of f_j. We will examine the creation of Steiner points on one edge e of f_j only. There are at most c more Steiner points added to e from each of the other ranges, where $c > 1$ is a constant. Furthermore, we will assume the worst case in which $|e| = |L|$. Figure 1.15 illustrates the important angles that arise when the Steiner points are added to f_j.

We will determine the length of $\delta_i, 0 \leq i \leq \iota$ and then determine ι. From the sine law:

$$\frac{x_i}{\sin\theta} = \frac{|L|}{\sin(\pi - (\theta+\beta))} = \frac{|L|}{\sin(\theta+\beta)}$$

Hence $x_i = \frac{|L|\sin\theta}{\sin(\theta+\beta)}$. Again using the sine law:

$$\frac{\delta_i}{\sin\lambda} = \frac{x_i}{\sin(\pi - (\lambda+\beta))} = \frac{x_i}{\sin(\lambda+\beta)}$$

Hence $\delta_i = \frac{|L|\sin\theta\sin\lambda}{\sin(\theta+\beta)\sin(\lambda+\beta)}$.

Now let $\Delta_0 = r$ and $\Delta_i = \sum_{j=0}^{i} \delta_j$, where $1 \le i \le \iota$ and let $f(\lambda, \theta, \beta) = \left(\frac{\sin\theta \sin\lambda}{\sin(\theta+\beta)\sin(\lambda+\beta)}\right)$. Then,

$$\begin{array}{l}
\Delta_i = |L|, \\
\Delta_{i-1} = \Delta_i - \delta_i = |L|(1 - f(\lambda, \theta, \beta)), \\
\Delta_{i-2} = \Delta_{i-1} - (\delta_{i-1}) = |L|(1 - f(\lambda, \theta, \beta))^2, \\
\dots \\
\Delta_0 = r
\end{array}$$

We would like to find a value for m such that $|L|(1 - f(\lambda, \theta, \beta))^m = r$. Let $\mathcal{F} = 1 - f(\lambda, \theta, \beta)$.

$$\begin{aligned}
\log_{\mathcal{F}}\left(\frac{r}{|L|}\right) &= \log_{\mathcal{F}}(\mathcal{F})^m \\
m &= \log_{\mathcal{F}}\left(\frac{r}{|L|}\right)
\end{aligned}$$

From this value of m, we see that as $\lambda \Rightarrow \infty$ or $\theta \Rightarrow \infty$, then $\mathcal{F} \Rightarrow 1$. We need to show that $0 < f(\lambda, \theta, \beta) < 1$. Clearly, $0 < f(\lambda, \theta, \beta)$ since $\beta + \theta + \lambda \le \pi$. We will show that

$$\begin{array}{rcl}
1 & < & \dfrac{\sin(\theta+\beta)\sin(\lambda+\beta)}{\sin\theta\sin\lambda} \\
 & < & \dfrac{(\sin\theta\cos\beta + \sin\beta\cos\theta)(\sin\lambda\cos\beta + \sin\beta\cos\lambda)}{\sin\theta\sin\lambda} \\
 & < & \dfrac{\cos^2\beta\sin\theta\sin\lambda + \sin\beta\cos\beta\sin\theta\cos\lambda + \sin^2\beta\cos\theta\cos\lambda + \sin\beta\cos\beta\cos\theta\sin\lambda}{\sin\theta\sin\lambda} \\
 & < & \cos^2\beta + \sin\beta\cos\beta\cot\lambda + \sin^2\beta\cot\theta\cot\lambda + \sin\beta\cos\beta\cot\theta \\
 & < & 1 - \sin^2\beta + \sin^2\beta\cot\theta\cot\lambda + \sin\beta\cos\beta\cot\lambda + \sin\beta\cos\beta\cot\theta
\end{array}$$

Since $\sin\beta > 0$, then we divide both sides by $\sin\beta$::

$$\begin{array}{rcl}
0 & < & \sin^2\beta(\cot\theta\cot\lambda - 1) + \sin\beta\cos\beta\cot\lambda + \sin\beta\cos\beta\cot\theta \\
0 & < & \sin\beta(\cot\theta\cot\lambda - 1) + \cos\beta\cot\lambda + \cos\beta\cot\theta
\end{array}$$

With some final maniupulation, we obtain:

$$\begin{array}{rcl}
\sin\beta\left(\dfrac{\cos\theta\cos\lambda - \sin\theta\sin\lambda}{\sin\theta\sin\lambda}\right) & > & -\cos\beta\left(\dfrac{\cos\lambda\sin\theta + \cos\theta\sin\lambda}{\sin\lambda\sin\theta}\right) \\
\sin\beta\cos(\theta+\lambda) & > & -\cos\beta\sin(\theta+\lambda) \\
0 & < & \sin\beta\cos(\theta+\lambda) + \cos\beta\sin(\theta+\lambda) \\
0 & < & \sin(\beta+\theta+\lambda) \\
\text{TRUE} & \text{since} & \beta+\theta+\lambda \le \pi.
\end{array}$$

For simplification, we will place an upper bound on β. In the worst case, $\mathcal{F}$ is minimized which implies that $f(\lambda, \theta, \beta)$ is maximized. To maximize $f(\lambda, \theta, \beta)$, we must minimize $\sin(\theta+\beta)\sin(\lambda+\beta)$.

Taking the derivative with respect to β allows use to transform the problem so that we need to prove $\cos(\beta+\theta)\sin(\beta+\lambda)+\cos(\beta+\lambda)\sin(\beta+\theta)=0$. We can expand this and group the terms differently as follows:

$$\begin{aligned}
0 &= \cos\beta\sin\beta\cos\lambda\cos\theta - \sin^2\beta\sin\theta\cos\lambda + \cos^2\beta\cos\theta\sin\lambda - \sin\beta\cos\beta\sin\theta\sin\lambda + \\
&\quad \cos\beta\sin\beta\cos\lambda\cos\theta - \sin^2\beta\cos\theta\sin\lambda + \cos^2\beta\cos\lambda\sin\theta - \sin\beta\cos\beta\sin\theta\sin\lambda \\
&= 2\cos\beta\sin\beta\cos\lambda\cos\theta - \sin^2\beta(\sin\theta\cos\lambda + \cos\theta\sin\lambda) + \\
&\quad \cos^2\beta(\cos\theta\sin\lambda + \cos\lambda\sin\theta) - 2\cos\beta\sin\beta\sin\theta\sin\lambda \\
&= 2\cos\beta\sin\beta\cos\lambda\cos\theta - 2\sin\beta\cos\beta\sin\theta\sin\lambda + (2\cos^2\beta - 1)\sin(\lambda+\theta) \\
&= 2\cos\beta\sin\beta\cos(\lambda+\beta) + (2\cos^2\beta - 1)\sin(\lambda+\theta) \\
&= \sin 2\beta\cos(\lambda+\theta) + \cos 2\beta\sin(\lambda+\theta) \\
&= \sin(2\beta+\lambda+\theta)
\end{aligned}$$

The only valid case is when $2\beta+\lambda+\theta=\pi$. This implies that $\beta=\pi/2-(\lambda+\theta)/2$. If we make this substitution into $\mathcal{F}$ we obtain:

$$\begin{aligned}
\mathcal{F} &= 1 - \frac{\sin\theta\sin\lambda}{\sin(\pi/2-(\lambda+\theta)/2+\theta)\sin(\pi/2-(\lambda+\theta)/2+\lambda)} \\
&= 1 - \frac{\sin\theta\sin\lambda}{\sin(\pi/2-(\lambda-\theta)/2)\sin(\pi/2-(\theta-\lambda)/2)} \\
&= 1 - \frac{\sin\theta\sin\lambda}{\cos((\lambda-\theta)/2)\cos((\theta-\lambda)/2)} \\
&= 1 - \frac{\sin\theta\sin\lambda}{\cos^2((\theta-\lambda)/2)} \\
&= 1 - \frac{\sin\theta\sin\lambda}{\left(\frac{1+\cos(\theta-\lambda)}{2}\right)} \\
&= 1 - \frac{2\sin\theta\sin\lambda}{1+\cos(\theta-\lambda)} \\
&= \frac{1+\cos(\theta-\lambda)-2\sin\theta\sin\lambda}{1+\cos(\theta-\lambda)} \\
&= \frac{1+\cos\theta\cos\lambda+\sin\theta\sin\lambda-2\sin\theta\sin\lambda}{1+\cos(\theta-\lambda)} \\
&= \frac{1+\cos\theta\cos\lambda-\sin\theta\sin\lambda}{1+\cos(\theta-\lambda)} \\
&= \frac{1+\cos(\theta+\lambda)}{1+\cos(\theta-\lambda)}
\end{aligned}$$

□

Claim 1.5.4 *G has $O(n\log_\delta(|L|/r)+n\log_{\mathcal{F}}(r/|L|))$ vertices and $O(n(\log_\delta(|L|/r)+\log_{\mathcal{F}}(r/|L|))^2)$ edges, where $\mathcal{F}=\frac{1+\cos(\theta+\lambda)}{1+\cos(\theta-\lambda)}$*

Proof: Follows from applying Claim 1.5.3 to each edge of $\mathcal{P}$.

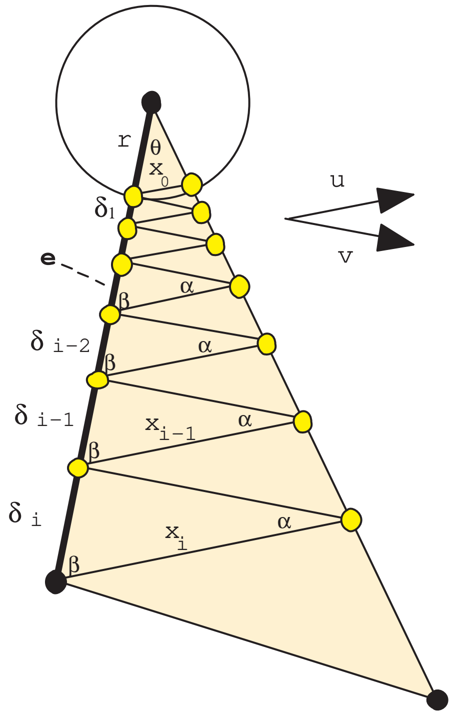

Figure 1.15: The angles defined during the creation of stage 2 Steiner points for a face f based on a sinlgee permissible range.

Lemma 1.5.1 *Let $\overline{ab}$ be the smallest segment contained within f_j such that one endpoint of $\overline{ab}$ intersects e_q between Steiner points q_i and q_{i+1} and the other endpoint intersects e_p, where q_i and q_{i+1} do not lie in any spheres C_v of f_j. It holds that $|\overline{q_i q_{i+1}}| \leq \epsilon|\overline{ab}|$. Furthermore, if $\theta_v < \frac{\pi}{2}$ then $\overline{ab}$ is a perpendicular to e_p and if $\theta_v \geq \frac{\pi}{2}$ then $|\overline{ab}| \geq |\overline{vq_i}|$.*

Proof: Consider first when $\theta_v < \frac{\pi}{2}$. Clearly, the smallest segment starting in the interval $[q_i, q_{i+1}]$ on e_q is a perpendicular to line e_p since e_q and e_p are not parallel. Furthermore, the smallest such perpendicular must start at q_i. Therefore $|\overline{ab}| \geq dist(q_i, e_p)$. Since Claim 1.5.1 ensures that $|\overline{q_i q_{i+1}}| = \epsilon \cdot dist(q_i, e_p)$, then $|\overline{q_i q_{i+1}}| \leq \epsilon|\overline{ab}|$. Now if $\theta_v \geq \frac{\pi}{2}$ then smallest segment starting in the interval $[q_i, q_{i+1}]$ on e_q is $\overline{vq_i}$. Therefore $|\overline{ab}| \geq |\overline{vq_i}| = dist(q_i, e_p)$. Once again, Claim 1.5.1 is used to show that $|\overline{q_i q_{i+1}}| \leq \epsilon|\overline{ab}|$. □

1.5.2 Constructing an Approximated Path

We describe here the construction of a path $\Pi'(s,t)$ in G which we will be bounding in the sections to follow. Note again that Dijkstra's algorithm may produce a better path than the one constructed here. As with the simple approximation scheme of Section 1.4, we will construct and bound the cost of $\Pi'(s,t)$. We do not describe the construction of $\Pi''(s,t)$ for reporting the path, although it is constructed similar to that from Section 1.4 and can be shown to have a finite number of segments. We begin with some preliminary notation and definitions.

Recall that a switchback path z_i of $\Pi(s,t)$ within face f_j is represented with a single segment (i.e. s_i) of $\Pi(s,t)$ whose weight encapsulates the distance of the switchback path. Each s_i, must be of one of the following types:

i) $s_i \cap C_v = \emptyset$,

ii) $s_i \cap C_v =$ subsegment of s_i, or

iii) $s_i \cap C_v = s_i$.

Let $C_{\sigma_1}, C_{\sigma_2}, ..., C_{\sigma_\kappa}$ be a sequence of spheres (listed in order from s to t) intersected by type ii) segments of $\Pi(s,t)$ such that $C_{\sigma_a} \neq C_{\sigma_{a+1}}$. Now define subpaths of $\Pi(s,t)$ as being one of two kinds:

Definition 1.5.1 Between-sphere subpath: *A path consisting of a type ii) segment followed by zero or more consecutive type i) segments followed by a type ii) segment. These subpaths will be denoted as $\Pi(\sigma_a, \sigma_{a+1})$ whose first and last segments intersect C_{σ_a} and $C_{\sigma_{a+1}}$, respectively. We will also consider paths that begin or/and end at a vertex to be a degenerate case of this type of path containing only type i) segments.*

Definition 1.5.2 Inside-sphere subpath: *A path consisting of one or more consecutive type iii) segments all lying within the same C_{σ_a}; these are denoted as $\Pi(\sigma_a)$. (Note that inside-sphere subpaths of $\Pi(s,t)$ always lie between two between-sphere subpaths. That is, $\Pi(\sigma_a)$ lies between $\Pi(\sigma_{a-1}, \sigma_a)$ and $\Pi(\sigma_a, \sigma_{a+1})$).*

Let x and y be the endpoints of s_i and let x (respectively y) lie on edge e_q (respectively e_p) of f_j. Let q_a and q_b (respectively p_a and p_b) be the Steiner points on e_q (respectively e_p) between which x (respectively y) lies.

Claim 1.5.5 *At least one of $\overrightarrow{q_a p_b}$ or $\overrightarrow{q_b p_a}$ is of the same direction type as s_i.*

Proof: Since s_i is an edge of $\Pi(s,t)$, it must travel in either a regular or braking direction (i.e. not impermissible). We will assume for this proof that it is braking and hence will show that at least one of $\overrightarrow{q_a p_b}$ and $\overrightarrow{q_b p_a}$ is also braking based on the Steiner points added in Stage 2. Note that the proof also applies in the case where s_i is regular since the Stage 2 Steiner points were made for those ranges as well. We will say that the critical angle directions for this range are $\vec{u}$ and $\vec{v}$. Let q'_a and q'_b be the closest Steiner points to x that were created in Stage 2 from the same range type as s_i. Let p'_a and p'_b be the Steiner points that were also created in Stage 2 (also same range type) via the extension of rays from q'_a in the directions $\vec{v}$ and $\vec{u}$, respectively. Similarly, let p''_a and p''_b be the Steiner points that were created in Stage 2 via the extension of a ray from q'_b in the directions $\vec{v}$ and $\vec{u}$, respectively (note that $p'_b = p''_a$). Figure 1.16 a) and b) show these Steiner points. It may be that $q_a = q'_a$ and/or $q_b = q'_b$. We will assume that these are not equal (as shown in the Figure), although the claim will still hold when either of these are equal. Now by construction of G during Stage 2, p_a and p_b must lie between either 1) p'_a and p'_b or 2) p''_a and p''_b as shown in the Figure. Consider the first case to be true and extend rays from q_a in the directions of $\vec{v}$ and $\vec{u}$. It is easily seen that $\overrightarrow{q_a p_b}$ lies between these rays and hence is of the same type as s_i. Consider now the second case to be true. We can extend similar rays from q_b and show that $\overrightarrow{q_b p_a}$ lies between these rays as well. Hence, at least one of $\overrightarrow{q_a p_b}$ or $\overrightarrow{q_b p_a}$ is of the same direction type as s_i. $\square$

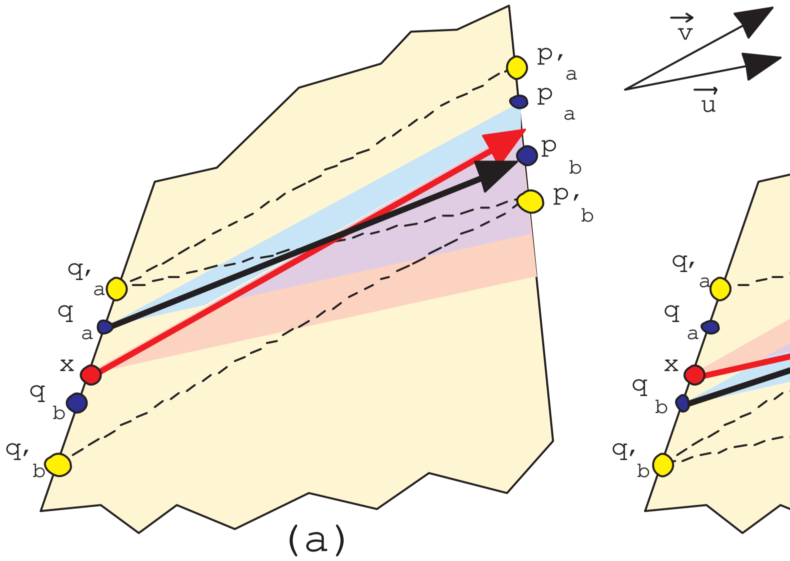

Figure 1.16: Example showing how s_i' is of the same direction type as s_i.

We begin our path construction by chosing a segment s_i' in G_j which approximates a segment s_i crossing face f_j. If s_i is a type i) or type ii) segment, then chose s_i' to be one of $\overrightarrow{q_a p_a'}$, $\overrightarrow{q_a p_b'}$, $\overrightarrow{q_b p_a'}$ and $\overrightarrow{q_b p_b'}$ such that s_i' is of the same direction type as s_i and $\|s_i'\|$ is minimized. Claim 1.5.5 ensures that at least one of these segments is of the same type as s_i. For the sake of analysis, we will assume that s_i' is chosen so as to have the same direction type as s_i and we will bound s_i' accordingly. In practice however, we may choose a segment with less cost, since we are choosing the minimum of these four. Note that this choice also pertains to the special case in which $e_q = e_p$. Note also that if s_i is of type ii), then one of q_a, q_b, p_a or p_b may degenerate to a vertex of f_j. In the case where s_i is a type iii) segment, there is no corresponding segment s_i' in $\Pi'(s,t)$.

At this point, we have approximations for all type i) and type ii) segments but they are disconnected and therefore do not form a path. We will now add edges joining consecutive type i) or type ii) segments of $\Pi(s,t)$. Let s_i and s_{i+1} be two consecutive segments of $\Pi(s,t)$ that are type i) or type ii) with corresponding approximation segments s_i' of G_j and s_{i+1}' of G_{j+1}, respectively. Let e be the edge of $\mathcal{P}$ joining faces f_j and f_{j+1}. Let q be the endpoint of s_i' lying on e and let p be the endpoint of s_{i+1}' lying on e. It is easily seen that either $q = p$ or q and p are adjacent Steiner points on e. If $q = p$, then s_i' and s_{i+1}' are already connected. If $q \neq p$ then let s_i'' be the edge in G_j from q to p. Figure 1.17 shows two examples of how s_i'' is used to connect s_i' and s_{i+1}'.

The addition of these segments (i.e. all s_i'') ensures that all segments of between-sphere subpaths are connected to form subpaths. We now need to interconnect the between-sphere subpaths so that $\Pi'(s,t)$ is connected.

Consider two consecutive between-sphere subpaths of $\Pi'(s,t)$, say $\Pi'(\sigma_{a-1},\sigma_a)$ and $\Pi'(\sigma_a,\sigma_{a+1})$. They are disjoint from one another, however, the first path ends at a Steiner point within sphere C_{σ_a} and the second path starts at a Steiner point within C_{σ_a}. Join the end of $\Pi'(\sigma_{a-1},\sigma_a)$ and the start of $\Pi'(\sigma_a,\sigma_{a+1})$ to vertex v_{σ_a} by two segments (which are edges of G created in Stage 3). These two segments together will form an inside-sphere subpath and will be denoted as $\Pi'(\sigma_a)$. This step

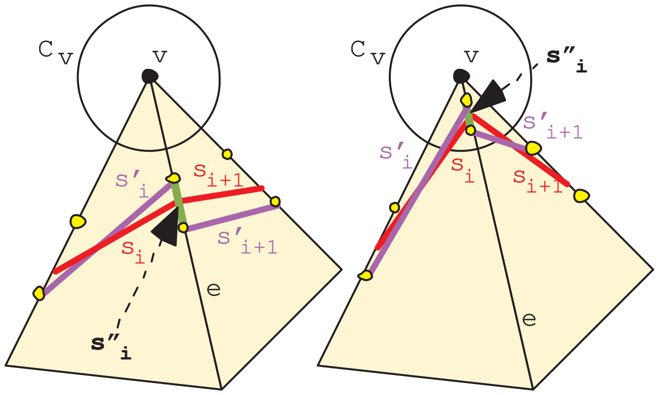

Figure 1.17: Examples showing the how segments s'_i and s'_{i+1} of $\Pi'(s,t)$ are connected via s''_i.

is repeated for each consecutive pair of between-sphere subpaths so that all subpaths are joined to form $\Pi'(s,t)$. (The example of Figure 1.18 shows how between-sphere subpaths are connected to inside-sphere subpaths.) Constructing a path in this manner results in a connected path that lies on the surface of $\mathcal{P}$.

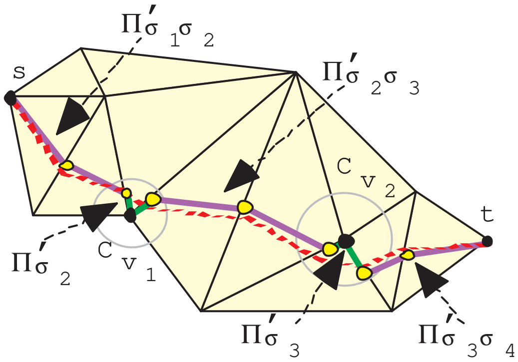

Figure 1.18: An example showing the between-sphere and inside-sphere subpaths that connect to form the approximated path $\Pi'(s,t)$.

1.5.3 Computing the ϵ-Approximation Bound

We give here a bound $\|\Pi'(s,t)\|$ on the cost of $\Pi'(s,t)$. To begin, a bound is shown for each of the between-sphere path segments. The claims to follow bound the approximation segments of the type i) and type ii) face crossing segments of $\Pi(s,t)$. Assume therefore that s'_i is a type i) or type ii) face-crossing segment. The claims give bounds for the three possible direction types of s'_i. That is, we bound the weighted cost of s'_i for the cases in which s'_i (and hence s_i) are regular, braking and switchback, respectively. Recall that x and y are the endpoints of s_i and that x (respectively y) lies on edge e_q (respectively e_p) of f_j. Also recall that q_a and q_b (respectively p_a and p_b) are the Steiner points on e_q (respectively e_p) between which x (respectively y) lies. In the proofs of these claims, we will assume that $s'_i = \overline{q_a p_b}$; similar proofs hold when $s'_i = \overline{q_b p_a}$.

Claim 1.5.6 *If s_i and s'_i are regular then $\|s'_i\| \le (1+2\epsilon)\|s_i\|$*

Proof: Through triangle inequality, we can state that: $|s'_i| \le |\overline{q_a x}| + |s_i| + |\overline{y p_b}|$. Now since Claim 1.5.5 ensures that s'_i is regular, then $\|s'_i\| = w_j|s'_i|$ and $\|s_i\| = w_j|s_i|$ and so

$$\begin{aligned}\frac{\|s'_i\|}{w_j} &\le |\overline{q_a x}| + \frac{\|s_i\|}{w_j} + |\overline{y p_b}| \\ &\le |\overline{q_a q_b}| + \frac{\|s_i\|}{w_j} + |\overline{p_a p_b}|.\end{aligned}$$

Lemma 1.5.1 ensures that $|\overline{q_a q_b}| \le \epsilon|s_i|$ and $|\overline{p_a p_b}| \le \epsilon|s_i|$. Therefore,

$$\begin{aligned}\frac{\|s'_i\|}{w_j} &\le 2\epsilon|s_i| + \frac{\|s_i\|}{w_j} \\ &= (1+2\epsilon)\frac{\|s_i\|}{w_j}.\end{aligned}$$

and so $\|s'_i\| \le (1+2\epsilon)\|s_i\|$. □

Claim 1.5.7 *If s_i and s'_i are braking then $\|s'_i\| \le \left(1+\frac{2\epsilon}{w_j}\right)\|s_i\|$, where w_j is weight of the face through which s_i and s'_i pass.*

Proof: First, examine the maximum possible height difference between s_i and s'_i. It is easily seen that $-\sin\varphi'_i|s'_i| \le -\sin\varphi_i|s_i| + |\overline{q_a q_b}| + |\overline{p_a p_b}|$.

Now since Claim 1.5.5 ensures that s'_i is braking, we can replace the terms above with the weighted costs $\|s'_i\|$ and $\|s_i\|$. Also, by using Lemma 1.5.1, we can show that $|\overline{q_a q_b}|$ and $|\overline{p_a p_b}|$ are at most $\epsilon|s_i|$ each. Therefore,

$$\begin{aligned}\|s'_i\| &\le \|s_i\| + 2\epsilon|s_i| \\ &= \|s_i\| + \frac{2\epsilon\|s_i\|}{-\sin\varphi_i} \\ &= (1+\frac{2\epsilon}{-\sin\varphi_i})\|s_i\|.\end{aligned}$$

Now the minimum possible value of $-\sin\varphi_i$ is at the critical braking angles (i.e. when $-\sin\varphi_i = w_j$). Therefore, $\|s'_i\| \le (1+\frac{2\epsilon}{w_j})\|s_i\|$. □

Claim 1.5.8 *If s_i and s'_i are switchback then $\|s'_i\| \le \left(1+\frac{2\epsilon}{\sin\frac{\alpha}{2}}\right)\|s_i\|$*

Proof: Figure 1.19 shows segments s_i and s'_i along with their corresponding switchback paths $z_i = z_{xy}$ and $z'_i = z_{q_a p_b}$. It is easily seen that

$$|z_{q_a p_b}| = |z_{q_a x}| + |z_{xy}| + |z_{y p_b}|.$$

We can put an upper bound on $|z_{q_a x}|$ and $|z_{y p_b}|$ as follows:

$$\begin{aligned} |z_{q_a p_b}| &\leq |z_{q_a q_b}| + |z_{xy}| + |z_{p_a p_b}| \\ &\leq \frac{|\overline{q_a q_b}|}{\sin\frac{\alpha}{2}} + |z_{xy}| + \frac{|\overline{p_a p_b}|}{\sin\frac{\alpha}{2}}. \end{aligned}$$

Now from Lemma 1.5.1 we are ensured that $|\overline{q_a q_b}| \leq \epsilon|\overline{xy}|$ and $|\overline{p_a p_b}| \leq \epsilon|\overline{xy}|$. We can therefore make this substitution:

$$\begin{aligned} |z_{q_a p_b}| &\leq \frac{|\overline{xy}|}{\sin\frac{\alpha}{2}}\epsilon + |z_{xy}| + \frac{|\overline{xy}|}{\sin\frac{\alpha}{2}}\epsilon \\ &= \frac{2|\overline{xy}|}{\sin\frac{\alpha}{2}}\epsilon + |z_{xy}| \\ &\leq \frac{2|z_{xy}|}{\sin\frac{\alpha}{2}}\epsilon + |z_{xy}| \\ &= \left(1 + \frac{2\epsilon}{\sin\frac{\alpha}{2}}\right)|z_{xy}|. \end{aligned}$$

Now $\|s_i'\| = w_j|z_{q_a q_b}|$ and $\|s_i\| = w_j|z_{xy}|$ so

$$\frac{\|s_i'\|}{w_j} \leq \left(1 + \frac{2\epsilon}{\sin\frac{\alpha}{2}}\right)\frac{\|s_i\|}{w_j}.$$

which leads to

$$\|s_i'\| \leq \left(1 + \frac{2\epsilon}{\sin\frac{\alpha}{2}}\right)\|s_i\|.$$

□

Claim 1.5.9 $\|s_i''\| \leq \frac{\epsilon}{\sin\frac{\alpha}{2}}\|s_i\|$.

Proof: By definition, s_i'' joins adjacent Steiner points on an edge of $\mathcal{P}$. Hence, from Lemma 1.5.1, it follows that $|s_i''| \leq \epsilon|s_i|$. Now it may be that s_i'' is impermissible, resulting in $\|s_i''\| \leq \frac{w_j}{\sin\frac{\alpha}{2}}|s_i''|$. Thus,

$$\|s_i''\| \leq \frac{w_j\epsilon}{\sin\frac{\alpha}{2}}|s_i|. \tag{1.4}$$

Now if s_i is regular or switchback, then it is easily shown that $|s_i| \leq \frac{\|s_i\|}{w_j}$. If s_i is braking, then $|s_i| = \frac{\|s_i\|}{-\sin\varphi_i} \leq \frac{\|s_i\|}{w_j}$. Thus, we can say that $|s_i| \leq \frac{\|s_i\|}{w_j}$.

Making this substitution into equation 1.4 results in $\|s_i''\| \leq \frac{w_j\epsilon}{\sin\frac{\alpha}{2}}\frac{\|s_i\|}{w_j} = \frac{\epsilon}{\sin\frac{\alpha}{2}}\|s_i\|$. □

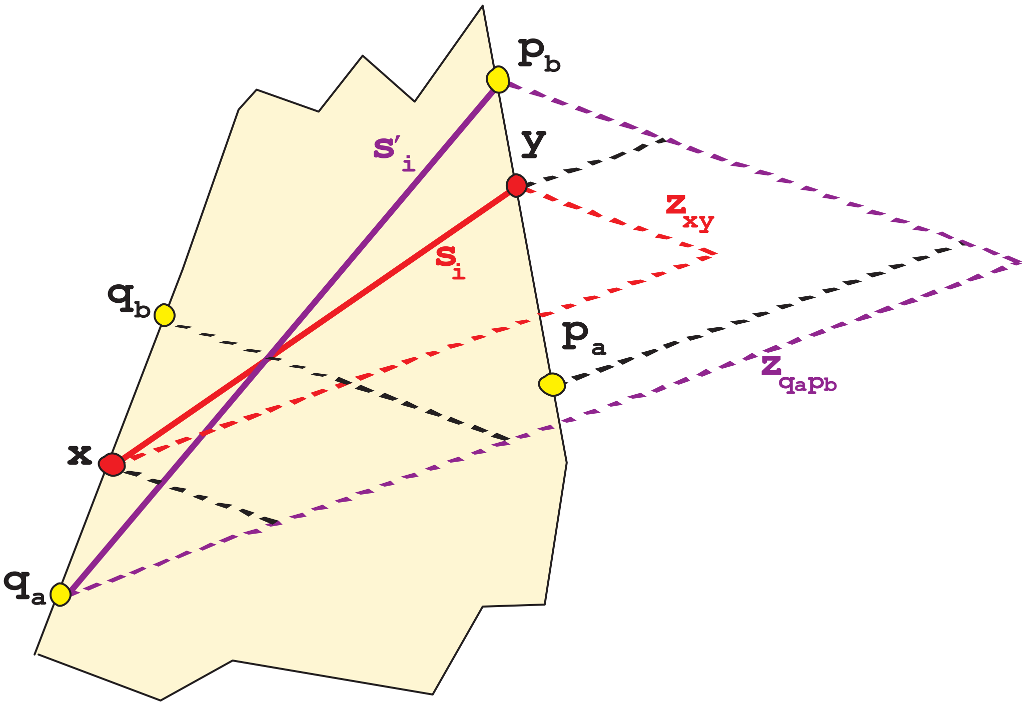

Figure 1.19: The switchback paths z_{xy} and $z_{q_a p_b}$ corresponding to segments s_i and s'_i, respectively.

Lemma 1.5.2 *If $\Pi'(\sigma_{a-1}, \sigma_a)$ is a between-sphere subpath of $\Pi'(s,t)$ corresponding to an approximation of $\Pi(\sigma_{a-1}, \sigma_a)$ then $\|\Pi'(\sigma_{a-1}, \sigma_a)\| \le (1 + \max(\frac{1}{\sin\frac{\alpha}{2}} + \frac{2}{w}, \frac{3}{\sin\frac{\alpha}{2}})\epsilon)\|\Pi(\sigma_{a-1}, \sigma_a)\|$, where w is the minimum weight of the faces of $\mathcal{P}$.*

Proof: Let s'_i be a segment of $\Pi'(\sigma_{a-1}, \sigma_a)$ which approximates a segment s_i of $\Pi(\sigma_{a-1}, \sigma_a)$ passing through face f_j. By Claims 1.5.6 1.5.7 and 1.5.8 we have

$$\begin{aligned}
\|s'_i\| &\le \max(1 + 2\epsilon, 1 + \frac{2\epsilon}{w_j}, 1 + \frac{2\epsilon}{\sin\frac{\alpha}{2}})\|s_i\| \\
&= (1 + 2\epsilon\max(1, \frac{1}{w_j}, \frac{1}{\sin\frac{\alpha}{2}}))\|s_i\| \\
&\le (1 + 2\epsilon\max(\frac{1}{w}, \frac{1}{\sin\frac{\alpha}{2}}))\|s_i\|
\end{aligned}$$

We can charge the cost of each s''_i to s'_i. Therefore, we can say from Claim 1.5.9 that

$$\begin{aligned}
\|s'_i\| + \|s''_i\| &\le (1 + 2\epsilon\max(\frac{1}{w}, \frac{1}{\sin\frac{\alpha}{2}}))\|s_i\| + \frac{\epsilon}{\sin\frac{\alpha}{2}}\|s_i\| \\
&= (1 + \epsilon(\frac{1}{\sin\frac{\alpha}{2}} + 2\max(\frac{1}{w}, \frac{1}{\sin\frac{\alpha}{2}})))\|s_i\| \\
&= (1 + \max(\frac{1}{\sin\frac{\alpha}{2}} + \frac{2}{w}, \frac{3}{\sin\frac{\alpha}{2}})\epsilon)\|s_i\|
\end{aligned}$$

Hence, each segment s_i' of $\Pi'(\sigma_{a-1},\sigma_a)$ has cost at most $(1+\max(\frac{1}{\sin\frac{\alpha}{2}}+\frac{2}{w},\frac{3}{\sin\frac{\alpha}{2}})\epsilon)\|s_i\|$ and $\|\Pi'(\sigma_{a-1},\sigma_a)\| \le (1+\max(\frac{1}{\sin\frac{\alpha}{2}}+\frac{2}{w},\frac{3}{\sin\frac{\alpha}{2}})\epsilon)\|\Pi(\sigma_{a-1},\sigma_a)\|$. □

Claim 1.5.10 *Let $\Pi'(\sigma_{a-1},\sigma_a)$ be a between-sphere subpath of $\Pi'(s,t)$ corresponding to an approximation of $\Pi(\sigma_{a-1},\sigma_a)$. Then $|\Pi'(\sigma_a)| \le \frac{2\epsilon}{1-2\epsilon}|\Pi(\sigma_{a-1},\sigma_a)|$, where $0<\epsilon<\frac{1}{2}$.*

Proof: From Property 1.5.1, the distance between $C_{\sigma_{a-1}}$ and C_{σ_a} must be at least $(1-2\epsilon)h_{v_{\sigma_a}}$. Since $\Pi(\sigma_{a-1},\sigma_a)$ is a between-sphere subpath, it intersects both $C_{\sigma_{a-1}}$ and C_{σ_a}. Thus $|\Pi(\sigma_{a-1},\sigma_a)| \ge (1-2\epsilon)h_{v_{\sigma_a}}$. By definition, $\Pi'(\sigma_a)$ consists of exactly two segments which together have length satisfying $|\Pi'(\sigma_a)| \le 2r_{v_{\sigma_a}} = 2\epsilon h_{v_{\sigma_a}}$. Thus, $|\Pi(\sigma_{a-1},\sigma_a)| \ge \left(\frac{1-2\epsilon}{2\epsilon}\right)|\Pi'(\sigma_a)|$ which can be re-written as $|\Pi'(\sigma_a)| \le \frac{2\epsilon}{1-2\epsilon}|\Pi(\sigma_{a-1},\sigma_a)|$. □

Claim 1.5.11 *Let $\Pi'(\sigma_{a-1},\sigma_a)$ be a between-sphere subpath of $\Pi'(s,t)$ corresponding to an approximation of $\Pi(\sigma_{a-1},\sigma_a)$ then $\|\Pi'(\sigma_a)\| \le \left(\frac{2W\epsilon}{w(1-2\epsilon)\sin\frac{\alpha}{2}}\right)\|\Pi(\sigma_{a-1},\sigma_a)\|$, where $0<\epsilon<\frac{1}{2}$.*

Proof: Claim 1.5.10 ensures that $|\Pi'(\sigma_a)| \le \frac{2\epsilon}{1-2\epsilon}|\Pi(\sigma_{a-1},\sigma_a)|$. In the worst case, we can assume that segments of $\Pi'(\sigma_a)$ are impermissible and that $\Pi(\sigma_{a-1},\sigma_a)$ is braking. Hence,

$$\begin{aligned}\|\Pi'(\sigma_a)\| &\le \frac{W}{\sin\frac{\alpha}{2}}|\Pi'(\sigma_a)| \\ &\le \frac{2W\epsilon}{(1-2\epsilon)\sin\frac{\alpha}{2}}|\Pi(\sigma_{a-1},\sigma_a)| \\ &\le \frac{2W\epsilon}{w(1-2\epsilon)\sin\frac{\alpha}{2}}\|\Pi(\sigma_{a-1},\sigma_a)\|.\end{aligned}$$

□

We have made the assumption that $\Pi'(\sigma_a)$ consists of segments passing through faces that have weight W. Although this may be true in the worst case, we could use the maximum weight of any face adjacent to v_{σ_a}, which typically would be smaller than W. In addition, we have assumed that $\Pi'(\sigma_{a-1},\sigma_a)$ traveled through faces with minimum weight. We could determine the smallest weight of any face through which $\Pi'(\sigma_{a-1},\sigma_a)$ passes and use that in place of w. This would lead to a better bound.

Lemma 1.5.3 *If $\Pi(s,p)$ is a shortest anisotropic path in $\mathcal{P}$, where s is a vertex of $\mathcal{P}$ and p is a vertex of G then there exists an approximated path $\Pi'(s,p)\in G$ such that*

$\|\Pi'(s,p)\| \le \left(1+\epsilon\left(\frac{2W\epsilon}{w(1-2\epsilon)\sin\frac{\alpha}{2}}+\max\left(\frac{1}{\sin\frac{\alpha}{2}}+\frac{2}{w},\frac{3}{\sin\frac{\alpha}{2}}\right)\right)\right)\|\Pi(s,p)\|$ *where $0<\epsilon<\frac{1}{2}$.*

Proof: Using the results of Claim 1.5.11 and Lemma 1.5.2, it can be shown that
$\|\Pi'(\sigma_{a-1},\sigma_a)\|+\|\Pi'(\sigma_a)\| \le \left(1+\epsilon\left(\frac{2W\epsilon}{w(1-2\epsilon)\sin\frac{\alpha}{2}}+\max\left(\frac{1}{\sin\frac{\alpha}{2}}+\frac{2}{w},\frac{3}{\sin\frac{\alpha}{2}}\right)\right)\right)\|\Pi(\sigma_{a-1},\sigma_a)\|$.
This essentially "charges" the length of an inside-sphere subpath to a between-sphere subpath. The union of all such subpaths form $\Pi'(s,p)$. This allows us to approximate $\Pi'(s,p)$ within the bound of $1+\epsilon\left(\frac{2W\epsilon}{w(1-2\epsilon)\sin\frac{\alpha}{2}}+\max\left(\frac{1}{\sin\frac{\alpha}{2}}+\frac{2}{w},\frac{3}{\sin\frac{\alpha}{2}}\right)\right)$ times the total cost of all the between-sphere subpaths of $\Pi(s,p)$. Since $\Pi(s,p)$ has cost at least that of its between-sphere subpaths, the lemma holds true. □

Corollary 1.5.1 *If $\Pi(s,t)$ is a shortest weighted path in $\mathcal{P}$, where s and t are vertices of $\mathcal{P}$ then there exists an approximated path $\Pi'(s,t) \in G$ such that*
$\|\Pi'(s,t)\| \le \left(1+\epsilon\left(\frac{2W\epsilon}{w(1-2\epsilon)\sin\frac{\alpha}{2}} + \max\left(\frac{1}{\sin\frac{\alpha}{2}}+\frac{2}{w}, \frac{3}{\sin\frac{\alpha}{2}}\right)\right)\right)\|\Pi(s,t)\|$ *where* $0<\epsilon<\frac{1}{2}$.

Proof: The proof follows from Lemma 1.5.3 since t is also a vertex of G. □

Theorem 1.5.1 *If $\mathcal{P}$ is a polyhedral surface such that $W \ge \sin\frac{\alpha}{2}$ and $\Pi(s,t)$ is a shortest weighted path in $\mathcal{P}$, where s and t are vertices of $\mathcal{P}$ then there exists an approximated path $\Pi'(s,t) \in G$ such that*
$\|\Pi'(s,t)\| \le \left(1+\epsilon\left(\frac{3W\epsilon}{w\sin\frac{\alpha}{2}}\right)\right)\|\Pi(s,t)\|$, *where* $0<\epsilon\le 3/8$.

Proof: The proof follows from Corollary 1.5.1. □

1.6 Extensions

One obvious improvement to the shortest energy path problem is that of restricting either the maximum allowable degree of each turn or the number of turns allowed in our approximation. The current approximations allow zig-zag paths which typically require sharp turns (possibly close to 180 degrees). For most vehicles, this is not possible. It would be more practical to produce paths that do not require these "sharp" turns. This would provide a more realistic solution that can be applied to real-world vehicles.

Some problems do arise, however, with this new constraint. With the previous model (which ignored turns), there was a possibility that for a given pair of points on $\mathcal{P}$, a valid path between them may not exist. With the added constraint on the turn angles, the probability of there being no valid path increases. The example of Figure 1.20 shows a valid switchback path between two points on a single face. The example shows the face with very steep slopes on the adjacent faces which may not allow traversal. Hence, if sharp turn angles are disallowed, no valid path exists between the two points shown.

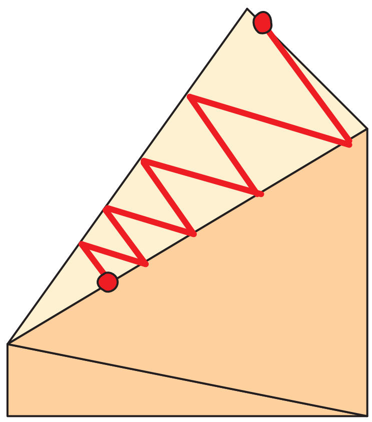

Figure 1.20: Example showing a switchback path between two points on a face. If the switchback path produces turns that are too sharp, there may be no valid path.

Assume now that given two points s and t on $\mathcal{P}$ that a valid path exists between them such that the turning constraint is also satisfied. In a sense, we are disallowing switchback paths within steep faces. This constraint produces a problem with our first algorithm since our approximated path segments are not of the same type as their corresponding shortest path segments. Hence, the existence of $\Pi(s,t)$ does not ensure the existence of a valid $\Pi'(s,t)$. In our second algorithm, we ensure that our approximated path segments are of the same type as the actual path segment which they approximate. However, our additional s'' segments that are used to join segments from consecutive faces may cause sharp turns. Therefore, the algorithm as stated, may not produce valid paths either.

Now intuitively, if we add more and more Steiner points to the edges of $\mathcal{P}$, then the chance of there being a valid turn path between s and t increases. However, it is non-trivial to determine the number of additional Steiner points that are required to ensure a path. It remains an open problem as to whether or not an efficient approximation can be produced for all valid $\Pi(s,t)$ paths when this additional turning constraint is added.

Bibliography

[1] L. Aleksandrov, M. Lanthier, A. Maheshwari and J.-R. Sack, "An ϵ-Approximation Algorithm for Weighted Shortest Path Queries on Polyhedral Surfaces", *14th European Workshop on Computational Geometry*, Barcelona, Spain, 1998.

[2] L. Aleksandrov, M. Lanthier, A. Maheshwari and J.-R. Sack, "An ϵ-Approximation Algorithm for Weighted Shortest Paths on Polyhedral Surfaces", *SWAT '98*, Stockholm, Sweden, 1998.

[3] H.S.M. Coxeter, "Introduction to Geometry", 2nd ed., published by John Wiley and Sons Inc., 1969, Ch. 13, pp. 198.

[4] M. Lanthier, A. Maheshwari and J.-R. Sack, "Approximating Weighted Shortest Paths on Polyhedral Surfaces", *Proc. of the 13th Annual Symp. on Computational Geometry*, Nice, France, June 4-6, 1997, pp. 274-283.

[5] J.S.B. Mitchell and C.H. Papadimitriou, "The Weighted Region Problem: Finding Shortest Paths Through a Weighted Planar Subdivision", *Journal of the ACM*, **38**, January 1991, pp. 18-73.

[6] N.C. Rowe and R.S. Ross, "Optimal Grid-Free Path Planning Across Arbitrarily Contoured Terrain with Anisotropic Friction and Gravity Effects", *IEEE Transactions on Robotics and Automation*, Vol. 6, No. 5, October 1990, pp. 540-553.

[7] A.A. Rula and C.J. Nuttall, "An Analysis of Ground Mobility Models(ANAMOB)", *Tech Report M-71-4*, U.S. Army Engineer Waterways Experiment Station, Vicksburg, MS, July 1971.